Mon. Not. R. Astron. Soc. **000**, 1–26 (2005) Printed 5 February 2008 (MN LATEX style file v2.2)

On the migration-induced resonances in a system of two planets with masses in the Earth mass range

J. C. B. Papaloizou[1,2] & E. Szuszkiewicz[3]
[1] *Astronomy Unit, Queen Mary, University of London, Mile End Rd, London E1 4NS, England,*
[2] *Department of Applied Mathematics and Theoretical Physics, Centre for Mathematical Sciences, Wilberforce Road, Cambridge CB3 0WA, United Kingdom*
[3] *Institute of Physics and CASA*, University of Szczecin, Wielkopolska 15, 70-451 Szczecin, Poland*

Accepted; Received; in original form

ABSTRACT

We investigate orbital resonances expected to arise when a system of two planets, with masses in the range 1-4 $M_\oplus$, undergoes convergent migration while embedded in a section of gaseous disc where the flow is laminar. We consider surface densities corresponding to $0.5-4$ times that expected for a minimum mass solar nebula at 5.2 AU. For the above mass range the planets undergo type I migration. Using hydrodynamic simulations we find that when the configuration is such that convergent migration occurs the planets can become locked in a first order commensurability for which the period ratio is $(p+1)/p$ with p being an integer and migrate together maintaining it for many orbits. Slow convergent migration results in commensurabilities with small p such as 1 or 2. Instead, when the convergent migration is relatively rapid as tends to occur for disparate masses, higher p commensurabilities are realized such as 4:3, 5:4, 7:6 and 8:7. However, in these cases the dynamics is found to have a stochastic character with some commensurabilities showing long term instability with the consequence that several can be visited during the course of a simulation. Furthermore the successful attainment of commensurabilities is also a sensitive function of initial conditions. When the convergent migration is slower, such as occurs in the equal mass case, lower p commensurabilities such as 3:2 are obtained which show much greater stability.

Resonant capture leads to a rise in eccentricities that can be predicted using a simple analytic model, that assumes the resonance is isolated, constructed in this paper. We find that, once the commensurability has been established, the system with an 8:7 commensurability is fully consistent with this prediction.

We find that very similar behaviour is found when the systems are modeled using an N body code with simple prescriptions for the disc planet interaction. Comparisons with the hydrodynamic simulations indicate reasonably good agreement with predictions for these prescriptions obtained using the existing semi-analytic theories of type I migration.

We have run our hydrodynamic simulations for up to $10^4 - 10^5$ orbits of the inner planet. Longer times could only be followed in the simpler N-body approach. Using that, we found that on the one hand an 8:7 resonance established in a hydrodynamic simulation could be maintained for more than 10^6 orbits. On the other hand other similar cases show instability leading to another resonance and ultimately a close scattering.

There is already one known example of a system with nearly equal masses in the several Earth mass range, namely the two pulsar planets in PSR B1257+12 which are intriguingly, in view of the results obtained here, close to a 3:2 commensurability. This will be considered in a future publication.

Future detection of other systems with masses in the Earth mass range that display orbital commensurabilities will give useful information on the role and nature of orbital migration in planet formation.

Key words: planet formation, migration, mean motion resonances

1 INTRODUCTION

The increasing number of extrasolar multi-planet systems, their diversity, and dynamical complexities provide a strong motivation to study the evolution and stability of such systems. One of the important features connected with planetary system evolution is the occurrence of mean motion resonances, which may relate to conditions at the time of or just after the process of formation. There are some well known examples of systems of celestial bodies exhibiting mean motion resonances both within our Solar System (Neptune and Pluto; Io, Ganymede and Europa (see eg. Goldreich, 1965)) and outside such as Gliese 876 (Marcy et al., 2001), HD 82943 (Mayor et al., 2004) and 55 Cancri (McArthur et al., 2004). As the latter examples involve planets with masses in the Jovian mass range, most of the investigations appropriate to extrasolar planets have focused on giant planets. However, it is likely that planetary systems around other stars may harbor planets with masses in the Earth mass range as well. These should be revealed by future space-based missions, such as Darwin, COROT, Kepler, SIM and TPF.

Meanwhile, it is important to establish the main features of the evolution of low mass planets embedded in a gaseous disc and in particular to determine the types of resonant configurations that might arise when a pair of such planets evolves together. The disc planet interaction naturally produces orbital migration through the action of tidal torques (Goldreich & Tremaine 1980; Lin & Papaloizou 1986) which in turn may lead to an orbital resonance in a many planet system eg. (Snellgrove, Papaloizou & Nelson 2001; Lee & Peale 2002). For low mass planets the disc undergoes small linear perturbations that induce density waves that propagate away from the planet. The angular momentum these waves transport away results in rapid orbital migration called type I migration (Ward 1997). In this type of migration, when the disc is laminar and inviscid, the planet is embedded and the surface density profile of the disc remains approximately unchanged. The rate of migration is proportional to mass of the planet and the timescale of inward migration on a circular orbit can be estimated for a disc with constant surface density to be given by (see Tanaka, Takeuchi & Ward (2002))

$$\tau_r = \left|\frac{r_p}{\dot{r}_p}\right| = W_m \frac{M_*}{m_{planet}} \frac{M_*}{\Sigma_p r_p^2} \left(\frac{c}{r_p \Omega_p}\right)^2 \Omega_p^{-1} \qquad (1)$$

Here M_* is the mass of the central star, m_{planet} is the mass of the planet orbiting at distance $r = r_p$, Σ_p is the disc surface density at $r = r_p$, c and Ω_p are the the local sound speed and angular velocity, Ω, at $r = r_p$ respectively. The numerical coefficient $W_m = 0.3704$.

It is important to note that type I migration appropriate to a laminar disc may lead to short migration times in standard model discs, that may threaten the survival of protoplanetary cores (Ward (1997)). However, in a disc with turbulence driven by the magnetorotational instability, the migration may be stochastic and accordingly less effective (Nelson & Papaloizou (2004)). Nonetheless there is considerable uncertainty as to the extent of turbulent regions in the disc resulting from uncertainties in the degree of ionization (eg. Fromang, Terquem & Balbus, 2002) so that type I migration appropriate to a laminar disc may operate in some regions. We also note that because it is inversely proportional to the disc surface density, the migration time becomes long in low surface density regions. Accordingly, for this first study of resonant interactions of planets in the mass range $1 - 30 M_\oplus$ embedded in a gaseous disc, we shall consider only migration induced by a laminar disc.

The density waves excited by a low mass planet with small eccentricity also lead to orbital circularization (eg. Artymowicz (1993); Papaloizou & Larwood (2000)) at a rate that can be estimated to be given by Tanaka & Ward (2004)

$$t_c = \frac{\tau_r}{W_c} \left(\frac{c}{r_p \Omega_p}\right)^2 . \qquad (2)$$

Here, the numerical coefficient $W_c = 0.289$.

It is expected from equation (1) that two planets with different masses will migrate at different rates. This has the consequence that their period ratio will evolve with time and may accordingly attain and, in the situation where the migration is such that the orbits converge, subsequently become locked in a mean motion resonance (eg. Nelson & Papaloizou (2002); Kley, Peitz & Bryden (2004)). In the simplest case of nearly circular and coplanar orbits the strongest resonances are the first-order resonances which occur at locations where the ratio of the two orbital periods can be expressed as the ratio of two consecutive integers, $(p+1)/p$, with p being an integer. As p increases, the two orbits approach each other and the strength of the resonance increases. In addition, the distance between successive resonances decreases as p increases. The combination of these effects ultimately causes successive resonances to overlap and so, in the absence of gas, leads to the onset of chaotic motion.

Resonance overlap occurs when the difference of the semi-major axes of the two planets is below a limit with half-width given, in the case of two equal mass planets, by Gladman (1993) as

$$\frac{\Delta a}{a} \sim \frac{2}{3p} \approx 2 \left(\frac{m_{planet}}{M_*}\right)^{2/7} , \qquad (3)$$

with a and m_{planet} being the mass and semi-major axis of either one of them respectively. Thus for a system consisting a two equal four Earth mass planets orbiting a central solar mass we expect resonance overlap for $p \gtrsim 8$. Conversely we might expect isolated resonances in which systems of planets can be locked and migrate together if $p \lesssim 8$.

However, note that the above discussion does not incorporate the torques producing convergent migration or eccentricity damping and thus may not give a complete account of the forms of chaos that might be expected. Kary, Lissauer & Greenzweig (1993) have discussed the case of small particles migrating towards a much more massive planet and indeed conclude that chaotic behaviour is more extensive in the non conservative case. This occurs because the higher p resonances can be unstable thus preventing long term trapping. The instability arises because, if locked in resonance, the orbit of a planet has some eccentricity. Making a slight perturbation to the orientation of the orbit produces an impulsive change to the semi-major axis at the next conjunction. This in turn affects the phase of the next conjunction and the next impulsive change to the semi-major axis. For resonances of high enough p this sequence results in instability and chaotic be-

haviour. Kary, Lissauer & Greenzweig (1993) give an estimate of when this form of instability occurs as

$$p > 0.667 \left(\frac{8\pi e m_{planet}}{3M_*} \right)^{-1/5}. \quad (4)$$

Here m_{planet}/M_* refers to the mass ratio for the most massive planet, and e is the orbital eccentricity for the planet with the smallest mass. Taking values appropriate to our simulations of $e \sim 0.04$, and $m_{planet}/M_* \sim 10^{-5}$, gives $p \gtrsim 8$. This is similar to the non dissipative estimate.

When this form of instability operates, long term stable trapping in commensurabilities is not possible. However, a system can remain in one for a long time before moving into another higher p commensurability. Furthermore detailed outcomes are very sensitive to input parameters, which is characteristic of chaotic motion. Slight changes can alter the sequence of commensurabilities a system resides in making the issue of their attainment acquire a probabilistic character. Both our hydrodynamic simulations and N body calculations show evidence of this behaviour. Although there may be islands of apparent stability, a system in this regime may ultimately undergo a scattering and exchange of the orbits of the two planets so that we should focus on stable lower p commensurabilities as being physically possible planetary configurations. The arguments given above suggest that these must have $p \lesssim 8$. Our calculations indicate that the limit is even smaller.

Hydrodynamic simulations of disc planet interactions, in which the discs are modelled as flat two dimensional objects with laminar flow governed by the Navier Stokes equations and which incorporate a migrating two giant planet system which evolves into a 2:1 commensurability have been performed by Kley (2000), Snellgrove, Papaloizou & Nelson (2001) and successfully applied to the GJ876 system. In addition to performing additional simulations, Papaloizou (2003) has developed an analytic model describing two planets migrating in resonance with arbitrary eccentricity. In this model the eccentricities are determined as a result of the balance between migration and orbital circularization. However, disc tides were considered to act on the outer planet only. Capture of giant planets into resonance has also been recently investigated numerically by Kley, Peitz & Bryden (2004).

In this paper we extend the types of two planet systems considered to include those with orbital resonances formed when the masses of the planets are $1-30M_\oplus$. Then for discs with aspect ratio $H/r = c/(r\Omega) \sim 0.05$ as in standard protostellar disc models, the orbital migration will be induced by type I migration.

In Section 2 we describe initial set up for our calculations giving the properties of the system in which two planets interact with each other and a gaseous disc.

In Section 3 we present the results of two dimensional numerical calculations showing how convergent differential migration of two planets can lead to resonance trapping followed by migration in which the resonance is maintained for the duration of the simulation which is characteristically around 2×10^4 orbits. By considering simulations with a range of planet masses and initial conditions, we are able to explore a variety of commensurabilities and show the sensitivity of the attainment of higher p commensurabilities to the input parameters, this being indicative of stochastic behaviour.

In Section 4 we compare our results with simplified N-body integrations which model the effects of the disc through the addition of terms to cause migration and eccentricity damping (see eg. Snellgrove, Papaloizou & Nelson (2001); Lee & Peale (2002); Adams & Laughlin (2003)). The comparison enables us to calibrate these terms and then apply the much faster N-body calculations to consider a wider range of planet masses and disc surface densities for a longer evolution time than is possible for the hydrodynamic simulations.

We summarize and discuss our results in the context of potentially observable commensurabilities in Section 6.

In addition, we generalize the analytic model of Papaloizou (2003) to incorporate migration and circularization effects for both planets and also to consider general first order commensurabilities in an Appendix. Thus this model can be applied to systems such as those considered here for which the planets have comparable mass and disc interactions may be important for either of them.

2 NUMERICAL SIMULATIONS OF MIGRATING PLANETS IN RESONANCE

We have performed simulations of two interacting planets together with an accretion disc with which they also interact. The simulations performed here are of the same general type as that performed by Snellgrove, Papaloizou & Nelson (2001) of the resonant coupling in the GJ876 system induced by orbital migration caused by interaction with the disc. For details of the numerical scheme and code adopted see Nelson et al. (2000). For the simulations performed here we adopt $n_r = 384$, and $n_\varphi = 512$ equally spaced grid points in the radial and azimuthal directions respectively.

We use a system of units in which the unit of mass is the central mass M_*, the unit of distance is the initial semimajor axis of the inner planet, r_2, and the unit of time is $2\pi(GM_*/r_2^3)^{-1/2}$, this being the orbital period on the initial orbit of the inner planet. When, as adopted below, r_2 corresponds to 1AU this unit of time is one year. In dimensionless units the inner boundary of the computational domain was at $r = r_{min} = 0.33$, and the outer boundary at $r = r_{max} = 4$. In all simulations, the disc model is locally isothermal with aspect ratio $H/r = 0.05$ and the kinematic viscosity is set to zero.

2.1 Initial configuration and computational set up

Our initial set up shown in Figure 1 includes the central star with a mass M_* and two orbiting planets with masses m_1 and m_2 respectively. The two planets are embedded in the disc which is a source of planet orbit migration. They are initialized on circular orbits with the central mass taken to have a fixed value of 1 solar mass. The gravitational potential was softened with softening parameter $b = 0.8H$. This results in the formation of an equilibrium atmosphere around the embedded planet which then does not accrete. This softening also allows an adequate representation of type I migration in two dimensional discs (see eg. Nelson & Papaloizou (2004)).

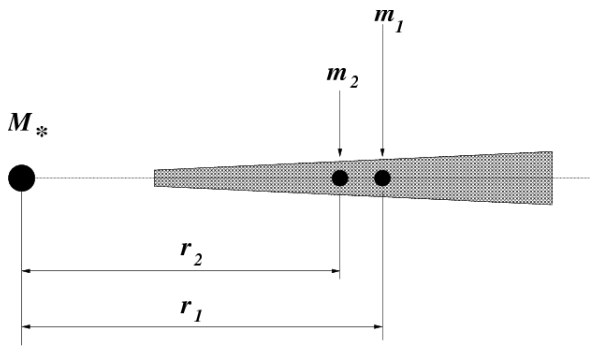

Figure 1. The initial configuration: two planets with masses m_1 and m_2, respectively, in circular orbit around a central star with mass M_* at distances r_1 and r_2 are embedded in a gaseous disc.

The disc in which planets are initially embedded has the initial surface density, $\Sigma(r)$, profile specified by

$$\Sigma(r) = \begin{cases} 0.1\Sigma_0(15(r-r_{min})/r_{min}+1) \text{ if } r \geqslant r_{min} \text{ and} \\ \quad r \leqslant 8r_{min}/5 \\ \Sigma_0 \text{ if } r > 8r_{min}/5 \text{ and} \\ \quad r < 4.5r_{min} \\ \Sigma_0\,(4.5r_{min}/r)^{1.5} \text{ if } r \geqslant 4.5r_{min} \end{cases}$$

where r_{min} is the inner edge of the computational domain. The planets are located in the flat part of this distribution. We use four different values for the maximum value of the surface density, Σ_0, namely $2\times10^3(5.2\mathrm{AU}/r_2)^2$ kg/m^2, the standard value attributed to the minimum mass solar nebula at 5.2AU which we denote Σ_1, then $\Sigma_{0.5}=0.5\Sigma_1$, $\Sigma_2=2\Sigma_1$ and finally $\Sigma_4=4\Sigma_1$. The radial boundaries were taken to be open.

3 TWO DIMENSIONAL HYDRODYNAMIC SIMULATIONS: A SURVEY

We have performed simulations of two interacting planets embedded in a disc with which they also interact. This interaction leads to spiral wave excitation, energy and angular momentum exchange between the planetary orbits and the gaseous disc which in turn results in orbital migration and eccentricity damping. We have carried out simulations for a variety of planet masses, initial orbital separations and initial surface density scaling in order to explore the possible outcomes. Because these simulations are very computationally demanding, the extent of the survey is limited. Nonetheless some characteristic features emerge. We describe some of these results below.

3.1 One pair of planets in three different resonances

In order to investigate how the orbital evolution depends on the surface density of the disc in which the planets are embedded we have considered two planets with masses $m_1=4M_\oplus$ and $m_2=1M_\oplus$. We assume that previous evolution brought the two planets to a configuration with circular orbits with $r_1/r_2=1.2$. This separation is slightly smaller than that required for a strict 4:3 commensurability. The faster migration expected for the outer planet (see equation (1)) will make the distance between the planets smaller and as a consequence of such convergent migration it is possible that they may become locked in a first order mean motion resonance (eg. Goldreich (1965)) such as 5:4, 6:5, 7:6, 8:7, ..., $(p+1):p$, ... and subsequently migrate together maintaining the commensurability for a considerable period of time or perhaps indefinitely, depending on how close the system is to a stochastic regime.

3.2 Attainment of commensurability

Papaloizou (2003) has given a simple approximate analytic solution for two migrating planets locked in a 2:1 commensurability. Only the outer planet was presumed to interact with the disc. As a result of the resonant interaction, the eccentricities of both planets grew with time until the effects of circularization due to disc tides balanced this. For the situation studied here, both planets are embedded in the disc and may have significant interaction with it. Furthermore, higher p commensurabilities than 2:1 occur for planet masses in the Earth mass range. Thus in the appendix we generalize the solution so that it applies to general first order commensurabilities and allows for disc tides to act on both planets. In particular we show that when the eccentricities stop growing, provided they are not too large, they must satisfy

$$\frac{e_1^2}{t_{c1}}+\frac{e_2^2}{t_{c2}}\frac{m_2n_1a_1}{m_1n_2a_2}-\left(\frac{e_1^2}{t_{c1}}-\frac{e_2^2}{t_{c2}}\right)f = \left(\frac{1}{t_{mig1}}-\frac{1}{t_{mig2}}\right)\frac{f}{3}, \quad (5)$$

where $f=m_2a_1/((p+1)(m_2a_1+m_1a_2))$.

Here the semi-major axes and eccentricities of the two planets ($i=1,2$) are a_i and e_i. The migration rates (assumed directed inwards) and circularization times induced by the disc tides are $t_{migi}=|n_i/\dot{n}_i|=|2a_i/(3\dot{a}_i)|=2\tau_r/3$, and $t_{ci}=|e_i/\dot{e}_i|$ respectively. The mean motions are n_i.

In addition near a $p+1:p$ resonance, the resonant angles $\phi=(p+1)\lambda_1-p\lambda_2-\varpi_1$, $\psi=(p+1)\lambda_1-p\lambda_2-\varpi_2$ and $\varpi_1-\varpi_2$ librate about equilibrium values which could be near to 0 or π mod 2π. Dissipative effects may be responsible for some shift. Here the mean longitudes and the longitudes of pericentre of the two planets ($i=1,2$) are λ_i and ϖ_i respectively. For giant planets like GJ876 these all librate about values close to zero. However, for lower mass planets the libration of $\varpi_1-\varpi_2$ in particular may be about π mod 2π (eg. Snellgrove, Papaloizou & Nelson (2001); Lee & Peale (2002)). All the simulations carried out here indicate libration about a value closer to π than 0.

Which resonance is established depends on the rate of relative migration. Roughly speaking one expects that locking occurs only if the relative migration is slow enough that the time to migrate through the resonance is longer that a characteristic libration period. The resonances become stronger as p increases, so that increasing the relative migration rate tends to cause the attainment of higher p commensurabilities. However, if the p becomes high enough ($p\sim8$ for the planet masses considered) the planets enter a chaotic region (see equations(3-4)) of phase space making commen-

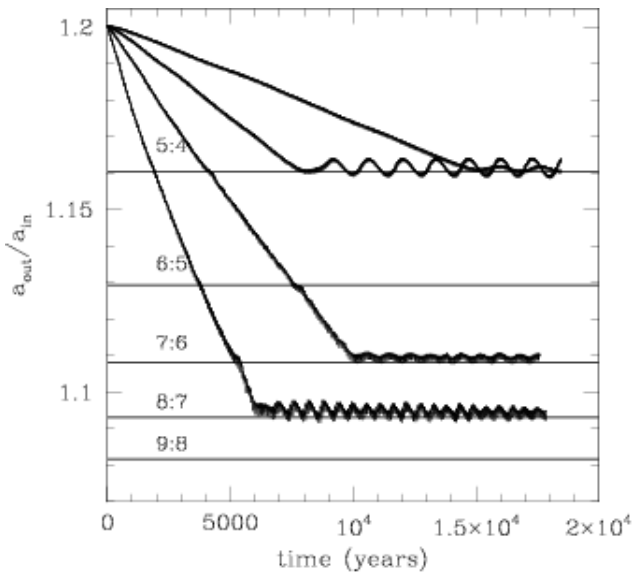

Figure 2. The evolution of the ratio of semi-major axes for the two planets with masses $m_1 = 4M_\oplus$ and $m_2 = 1M_\oplus$. Starting from the lower curve and going upwards the curves correspond to the initial surface density scalings $\Sigma_0 = \Sigma_4$, $\Sigma_0 = \Sigma_2$, $\Sigma_0 = \Sigma_1$, and $\Sigma_0 = \Sigma_{0.5}$ respectively.

surabilities unstable in the long term (although a system may remain in the vicinity of one for a considerable time) and introducing sensitivity of detailed outcomes to initial conditions. In such cases a scattering may ultimately occur that interchanges the positions of the planets. Thus very high surface densities with very rapid migration rates do not favour attainment of very stable commensurabilities.

In order to study these effects, we have considered the pair of planets evolving in discs with $\Sigma_0 = \Sigma_{0.5}$, $\Sigma_0 = \Sigma_1$, $\Sigma_0 = \Sigma_2$ and $\Sigma_0 = \Sigma_4$. The evolution was followed until a resonance was established. The results are summarized in Figure 2 where the evolution of the ratio of the semi-major axes, which starts from the value 1.2 for all four cases, is shown. The fastest migration (steepest slope) corresponds to the case where the two planets with $m_1 = 4M_\oplus$ and $m_2 = M_\oplus$ are embedded in a disc with $\Sigma_0 = \Sigma_4$ and the slowest to a case with a disc with $\Sigma_0 = \Sigma_{0.5}$. The planets in the disc with $\Sigma = \Sigma_4$ become trapped in 8:7 resonance. If the disc surface density is two times smaller then a 7:6 resonance is attained, if it is four or eight times smaller then the resonance attained is 5:4. These results are fully consistent with the idea that higher p resonances are associated with faster relative migration rates.

However, this situation corresponds to the evolution during first 18000 years and it is not obvious that the planets will remain in the same resonances in their subsequent evolution. This is because in addition to possibly being in a chaotic regime, the ratio of migration time to local orbital period varies with disc parameters and accordingly disc location. Consequently, the relative migration might become relatively faster as the evolution proceeds resulting in a shift to a higher p resonance. We comment that a slowing of relative migration, as long as it does not lead to a reversal, will not result in a transition to a lower p resonance. Therefore changes in effective local migration rates will tend to lead to higher p commensurabilities and ultimately chaos.

The whole evolution for the fastest migration rate is illustrated in Figure 3. We show there the evolution of the individual semi-major axes, eccentricities, angle between apsidal lines and one of the resonant angles. A surface density contour plot of the disc near the end of the simulation is given in Figure 3 together with a comparison between the initial and final surface density profiles.

The inner planet did not migrate significantly until 8:7 resonance was attained at about 6000 years. Subsequently the two planets migrated inwards together maintaining the commensurability. The system appears to be close to the chaotic regime as estimated by use of equations (3 - 4). During 18000 years of evolution the outer planet changed its location from a dimensionless radius of 1.2 to 0.9. The eccentricity of the outer planet increased slightly and that of the inner planet substantially, reaching at around 10000 years the balanced value of 0.04 and at later times oscillating around this value. At the end of simulation shown here the ratio of eccentricities, e_1/e_2, is equal to 0.125. The local peaks in the values of inner planet eccentricity occurring at 2000, 4000 and around 5400 years correspond to the planet passing through the 5:4, 6:5 and 7:6 resonances respectively. After about 8000 years the angle between the apsidal lines is oscillating around 212° and the resonant angle ϕ around 264°. The amplitude of the oscillations for both angles is decreasing with time. Similar behaviour can be seen in the evolution of these planets when embedded in a disc with lower surface density (see Figure 4).

When $\Sigma_0 = \Sigma_2$, leading to a slower rate of migration, as before, the inner planet did not migrate significantly until a commensurability was achieved and maintained. A 7:6 resonance was reached after 10000 years and subsequently maintained. The passage through the 5:4 and 6:5 commensurabilities are clearly marked by a local increase of inner planet eccentricity and also in behaviour of the angle between apsidal lines. In fact after the passage through 5:4 resonance the eccentricities do not completely decay potentially making the outcome of subsequent resonance passages probabilistic (Kary, Lissauer & Greenzweig 1993). In this case the planets relative migration is slower and the planets stay longer in the vicinity of these resonances. At the end of the evolution the eccentricities ratio is e_1/e_2 =0.14. The eccentricity of the inner planet is slightly higher than it was in the case with $\Sigma_0 = \Sigma_4$. However, the eccentricities continue to grow and the equilibrium is not quite established at the end of the simulation. The amplitude of oscillations in both the angle between the apsidal lines and the resonant angle ϕ, is smaller than in the previous case. For the two simulations that started with even lower disc surface densities such that $\Sigma_0 = \Sigma_1$ and $\Sigma_0 = \Sigma_{0.5}$, the evolution is shown in Figures 5-6.

When $\Sigma_0 = \Sigma_1$, the evolution of two planets leads to locking in 5:4 resonance. This happens at around 8000 years. Before that the inner planet migrated very slowly. After becoming trapped in the commensurability the inner planet semi-major axis changes in a characteristic oscillatory manner. These oscillations are clearly visible in all other related plots (eg. Figure 5). The eccentricity ratio at the end of the simulations is $e_1/e_2 = 0.18$. The eccentricities are still growing. Similar behaviour is seen in angle between the ap-

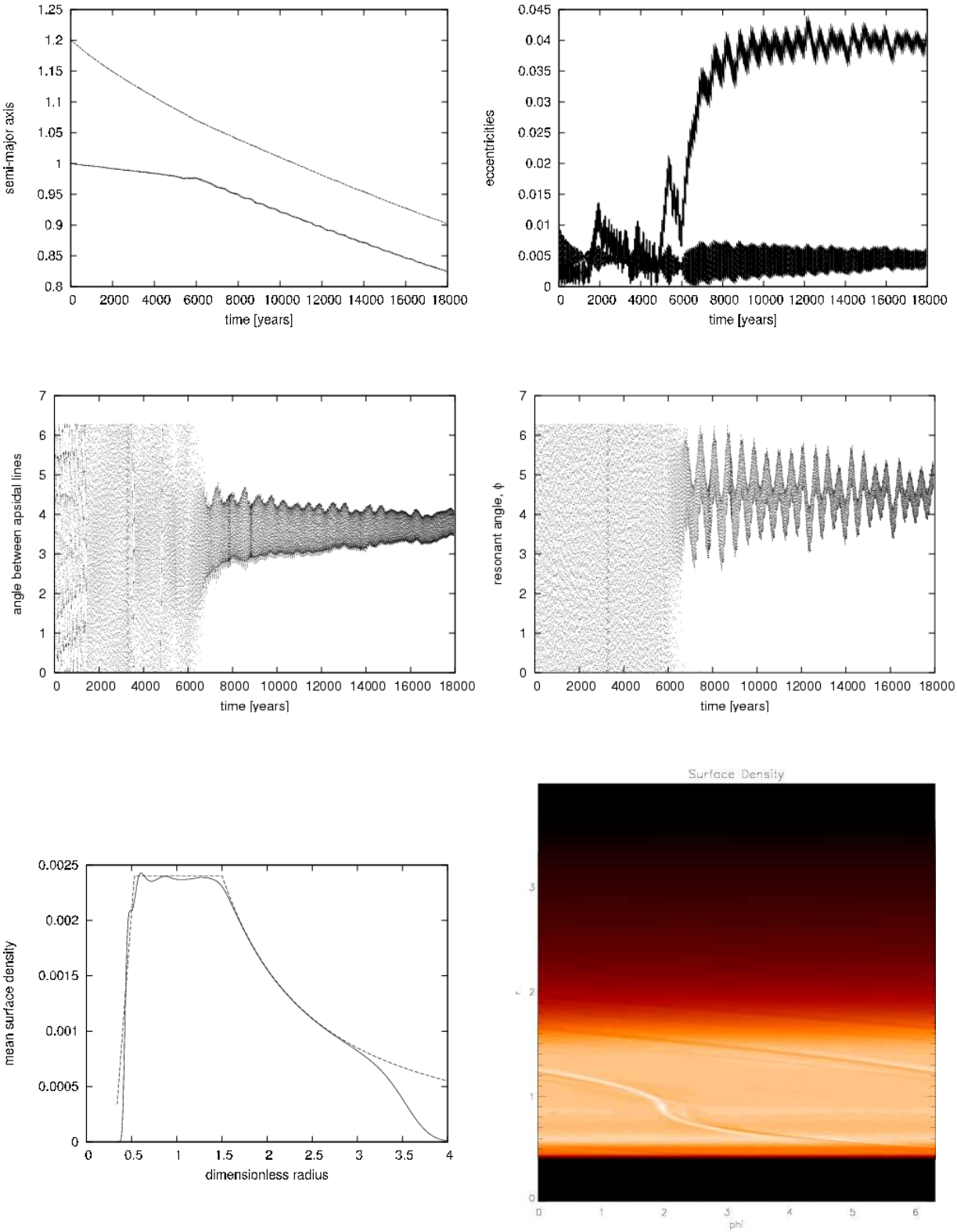

Figure 3. The evolution of the semi-major axes, eccentricities, angle between apsidal lines and the resonant angle for the two planets with masses, $m_1 = 4M_\oplus$ and $m_2 = M_\oplus$ migrating towards a central star, embedded in a disc with initial surface density scaling $\Sigma_0 = \Sigma_4$, obtained by hydrodynamical simulations (four upper panels). The mean surface density profile of the disc near the end of the simulation (solid line) and the initial surface density profile (dashed line) and a surface density contour plot are given in two lower panels.

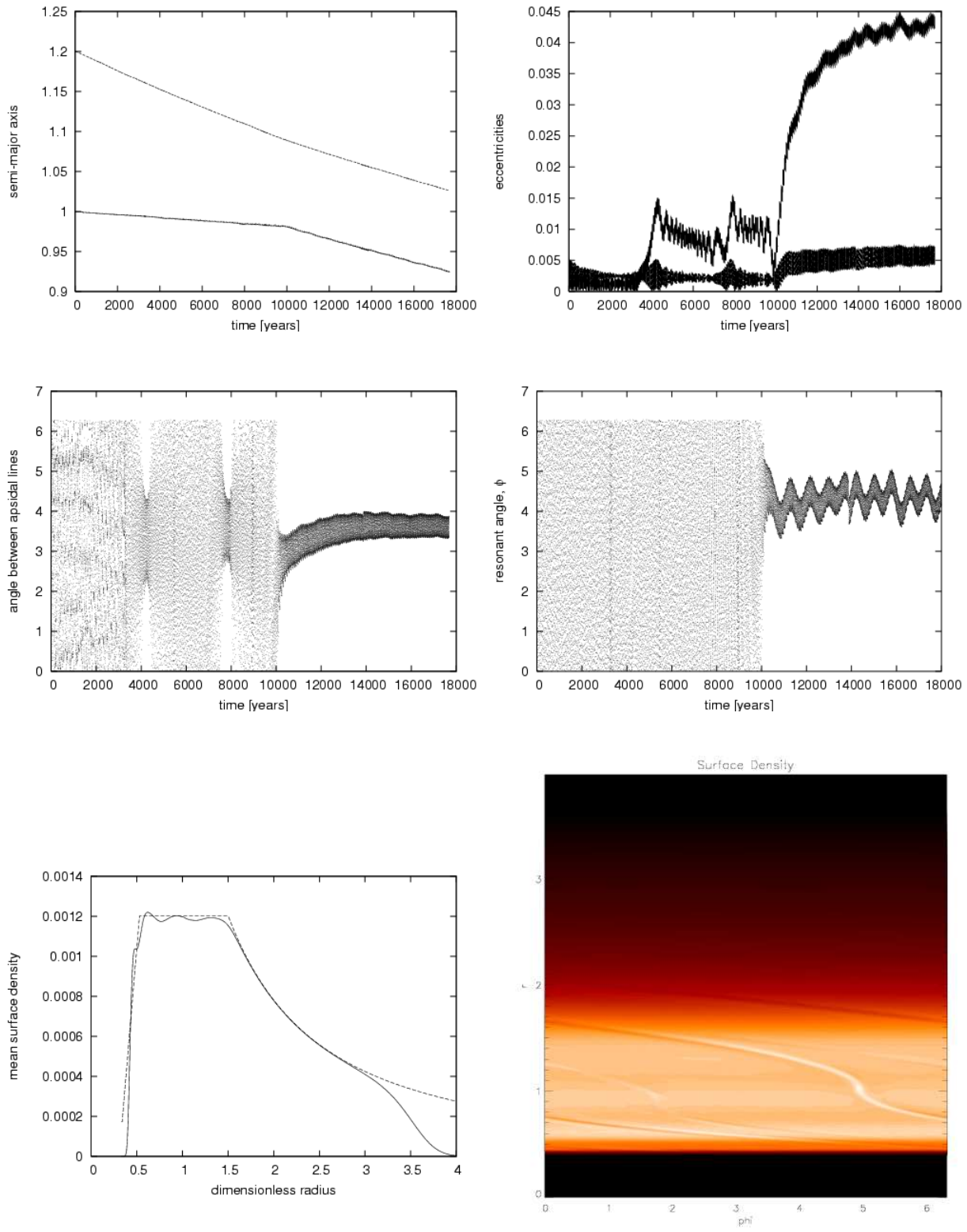

Figure 4. As for Figure 3 but when the planets are embedded in a disc with $\Sigma_0 = \Sigma_2$. Note the passage through the 5:4 and 6:5 resonances at $t \sim 4000$ and $t \sim 8000$ years respectively.

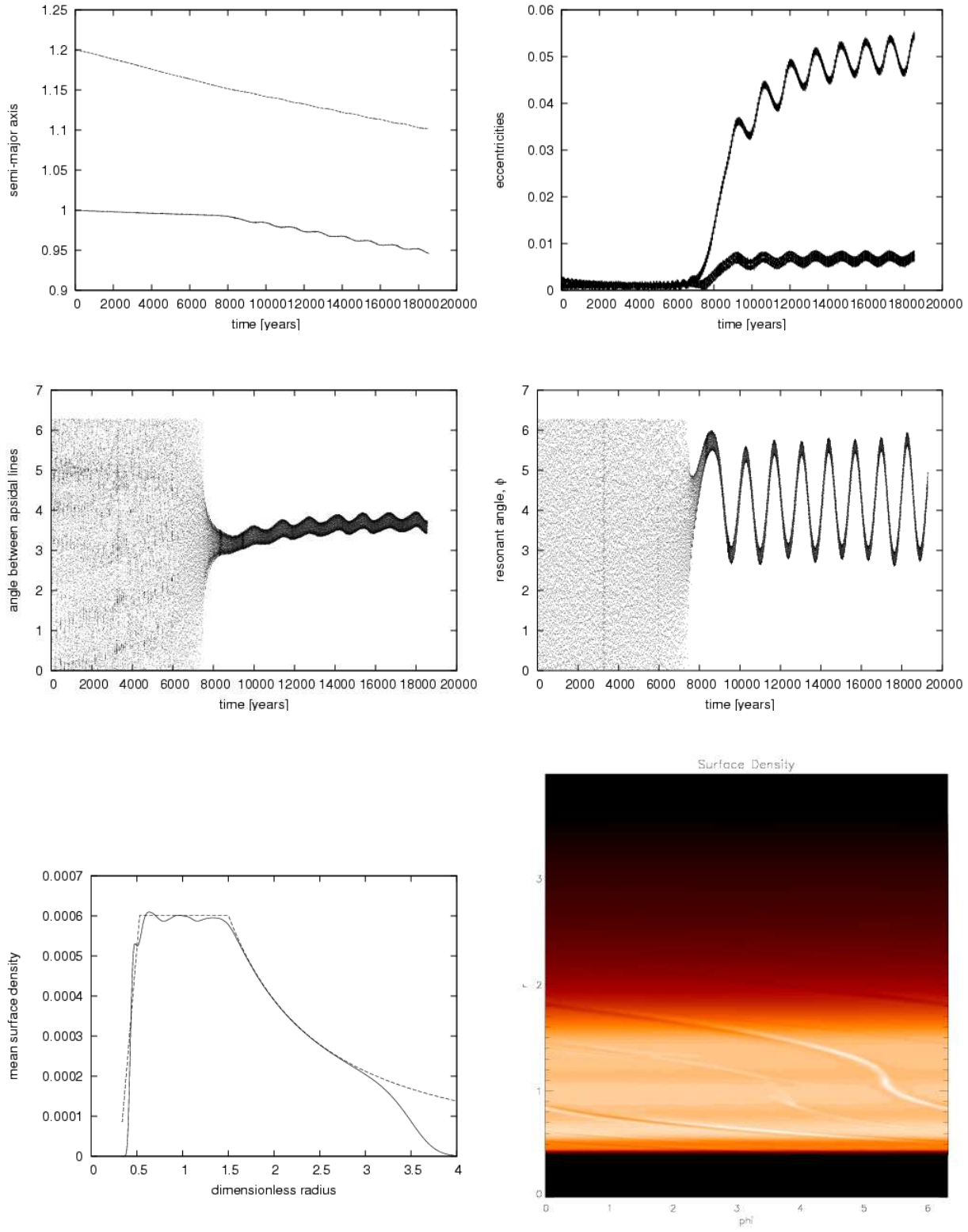

Figure 5. As for Figure 3 but for the case when the planets are embedded in the disc with initial surface density scaling $\Sigma_0 = \Sigma_1$.

sidal lines, which starts to librate at time 8000 years around 180° and at time 18000 years oscillates around 212°. The resonant angle changes have very large amplitude and seem to grow with time, which might indicate that the planets will not remain in this resonance. In this context note that equation (1) indicates that $t_{migi}n_i$ increases inwards for a uniform surface density. This should favour resonance locking at smaller radii.

Also the planets in a disc with $\Sigma_0 = \Sigma_{0.5}$ end in a 5:4 commensurability. It occurs after approximately 14000 years. Because of slow migration rates in low surface density discs, the subsequent evolution could not be continued for long enough to be able to make a definitive statement about the final outcome. However, the oscillations in the resonance angles are much smaller and more closely centred around π than is the case when $\Sigma_0 = \Sigma_1$. This could indicate greater stability of the 5:4 resonance in this case.

3.3 Comparison with the analytic model

It is of interest to compare the eccentricities obtained above when the planets are trapped in a commensurability with what is expected when resonant effects and disc tides are in balance. In the simple analytic model given in the appendix, when the eccentricities are small these satisfy equation (5). In principle orbital circularization acting on both planets should be included. However, for the simulations presented here, $e_2 >> e_1$ and even though the circularization time may be smaller for the possibly more massive outer planet, the effect can be neglected in comparison to that associated with the inner planet. Accordingly we set $e_1 = 0$. Then equation (5) gives the simple relation

$$\frac{e_2^2}{t_{c2}}\left(\frac{m_2 n_1 a_1}{m_1 n_2 a_2} + f\right) = \left(\frac{1}{t_{mig1}} - \frac{1}{t_{mig2}}\right)\frac{f}{3}, \qquad (6)$$

where we recall that $f = m_2 a_1/((p+1)(m_2 a_1 + m_1 a_2))$. We further simplify matters by assuming that p is large. Then we may set $a_1 = a_2, n_1 = n_2$ and neglect f on the left hand side of (6). In the same spirit, we replace it by $m_2/((p+1)(m_2+m_1))$ on the right hand side. Then we obtain

$$\frac{e_2^2}{t_{c2}} = \left(\frac{1}{t_{mig1}} - \frac{1}{t_{mig2}}\right)\frac{m_1}{3(p+1)(m_2+m_1)}, \qquad (7)$$

Interestingly equation (7) shows that it is the rate of convergent migration of the two planets that determines the eccentricities which are small when this is small in agreement with our results. Further, other things being equal, the eccentricities decrease with increasing p. We also note that use of equations (1) and (2) gives $t_c = (\tau_r/W_c)(H/r)^2$. Thus we obtain after recalling that in general the e folding rate for mean motion is a factor of 1.5 greater than that for radius, or $t_{mig} = 2\tau_r/3$

$$e_2^2 = \left(\frac{m_1}{m_2}\left(\frac{a_1}{a_2}\right)^{1/2} - 1\right)\frac{m_1}{0.578(p+1)(m_2+m_1)}(H/r)^2. \qquad (8)$$

We apply this to the case illustrated in Figure 3 for the two planets with masses, $m_1 = 4M_\oplus$ and $m_2 = M_\oplus$ embedded in a disc with initial surface density scaling $\Sigma_0 = \Sigma_4$ and obtain $e_2 = 0.037$ in reasonable agreement with the simulations.

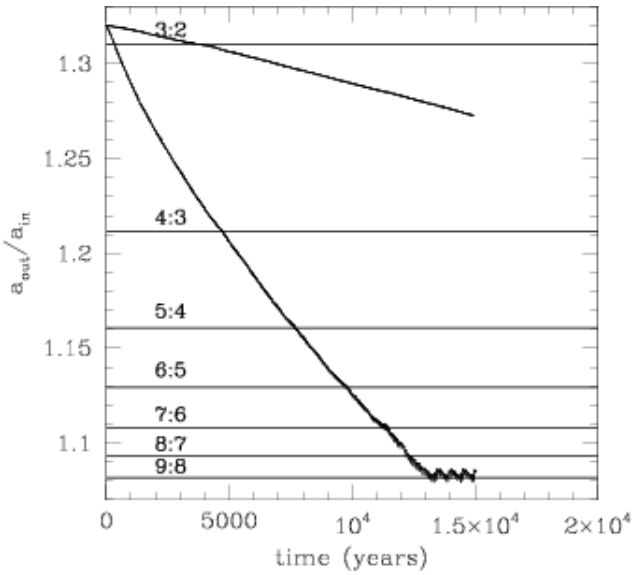

Figure 7. The semi-major axis ratio when $m_1 = 4M_\oplus$, $m_2 = 1M_\oplus$ with $\Sigma_0 = \Sigma_{0.5}$ - upper curve and $\Sigma_0 = \Sigma_4$ - lower curve.

3.4 Dependence on the initial separation of the planets

Here we investigate the dependence of attained commensurabilities on the initial radial separation of the planets. To do this we have performed simulations with planets of the same mass as above but starting with orbital separations a little larger than that required for strict 3:2 and 4:3 commensurabilities. In the former case the two planets were initiated with $r_1 = 1.32$ and $r_2 = 1.00$. Two initial surface density scalings were considered, namely $\Sigma_0 = \Sigma_{0.5}$ and $\Sigma_0 = \Sigma_4$. The evolution of the ratio of the semi-major axis ratios for both cases is plotted in Figure 7. For $\Sigma_0 = \Sigma_4$ the end state has the planets in a 9:8 resonance. The evolution for $\Sigma_0 = \Sigma_{0.5}$ is shown for comparison. The result in the $\Sigma_0 = \Sigma_4$ case is a clear indication that the system gets into the chaotic regime as a value of p of the attained resonance is increased when the initial semi-major axis ratio was larger. Stability would have implied that the same resonance should have been attained. Unfortunately the migration rate in the $\Sigma_0 = \Sigma_{0.5}$ case was too slow for us to be able to attain a commensurability with the available computational resources and confirm or otherwise the stability of the 4:3 commensurability.

When the ratio of the initial semi-major axes is changed from 1.2 to 1.32 the two planets embedded in a disc with $\Sigma_0 = \Sigma_4$ become trapped in a different resonance (compare Figure 3 and Figure 8). This is again consistent with the presence of stochastic behaviour as a different migration history leads to different end states and it suggests that having crossed different resonances before attaining a current one may influence the final outcome.

A similar experiment has been performed but now placing the planets close to 4:3 resonance. In this case we have chosen discs with lower surface density, such that $\Sigma_0 = \Sigma_{0.5}$ and $\Sigma_0 = \Sigma_1$. In the former case the system enters into 4:3 resonance while in the latter the system passes through the 4:3 resonance and becomes trapped in the 6:5 resonance.

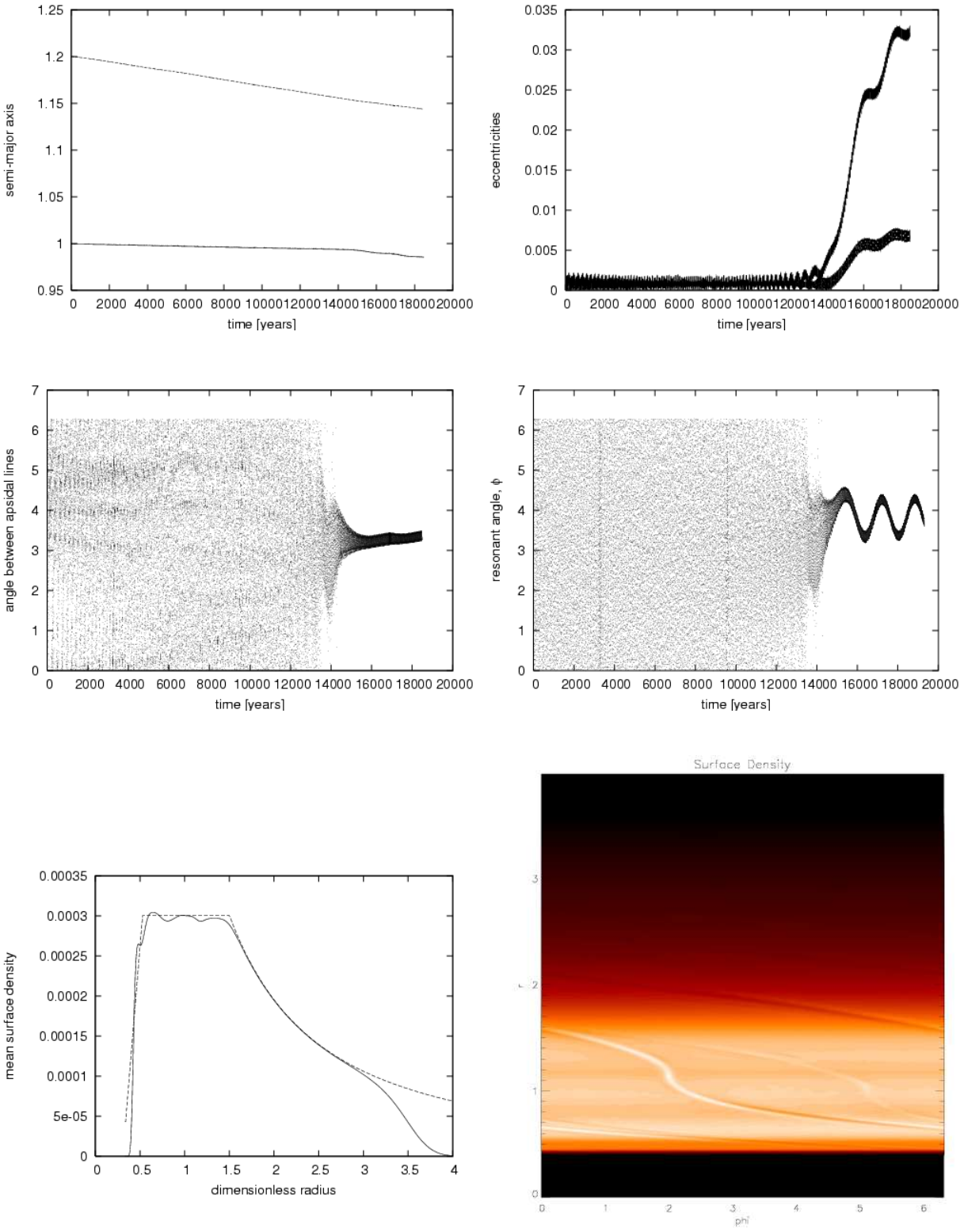

Figure 6. As for Figure 3 but for the case when the planets are embedded in a disc with $\Sigma_0 = \Sigma_{0.5}$.

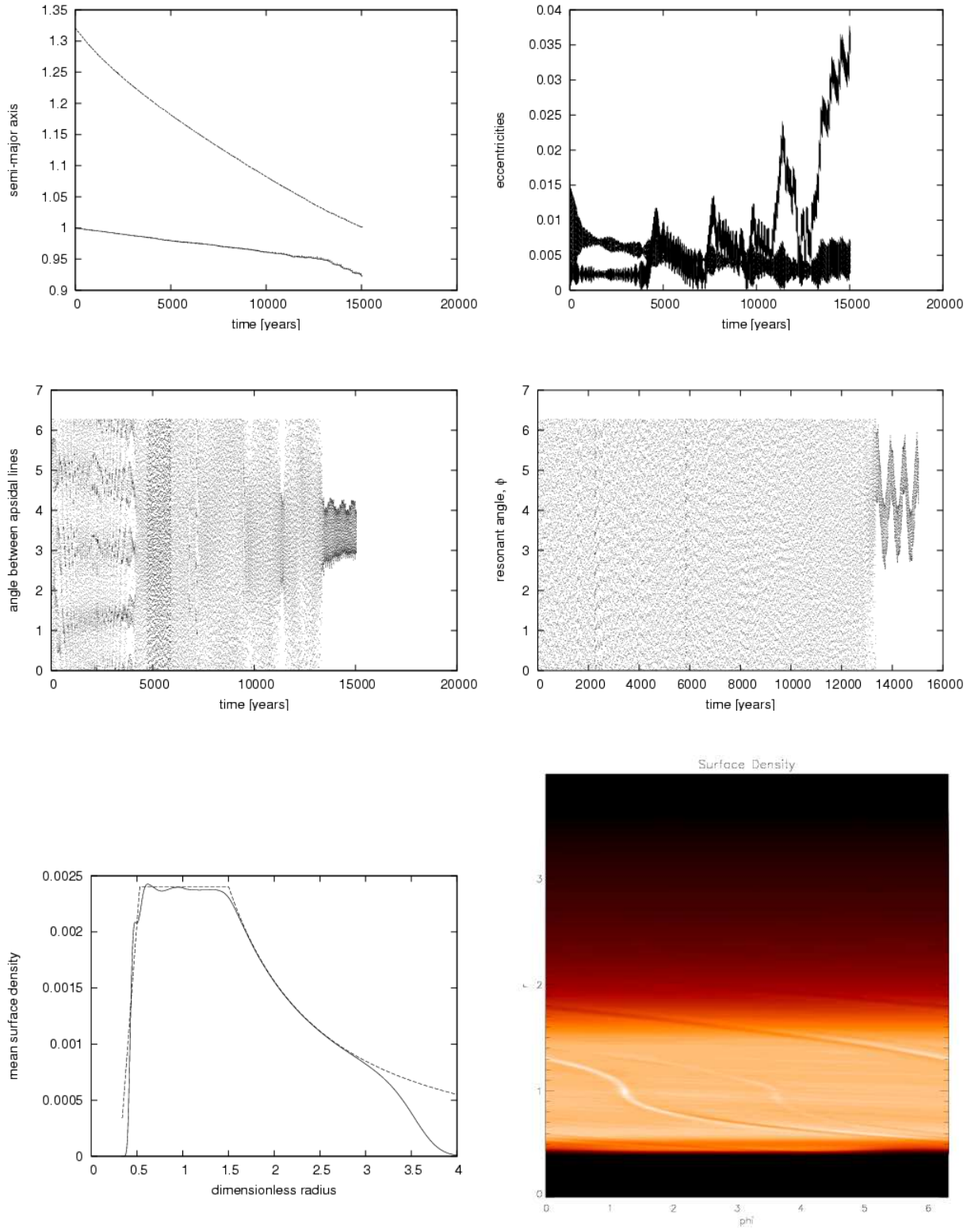

Figure 8. As for Figure 3 but here the planets initially have $a_1/a_2 = 1.32$. This system ended up in a 9:8 commensurability. Note the eccentricity increases produced by prior resonance passages which do not completely decay between them.

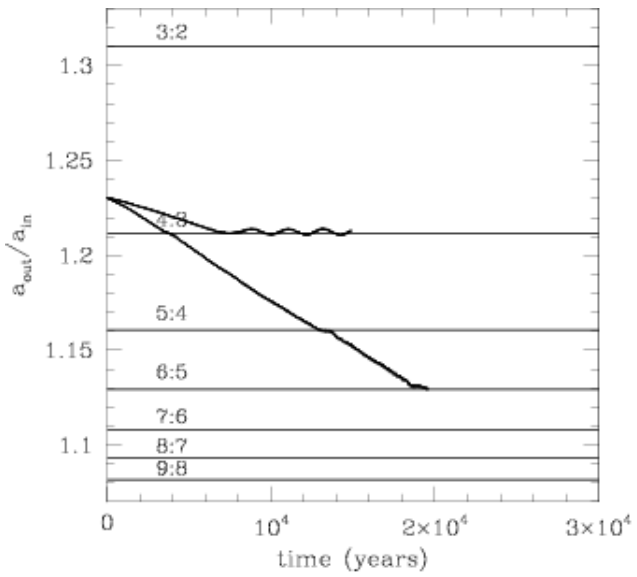

Figure 9. The semi-major axis ratio for $m_1 = 4M_\oplus$ and $m_2 = 1M_\oplus$ with surface density scaling parameter $\Sigma_0 = \Sigma_{0.5}$ - upper curve and $\Sigma_0 = \Sigma_1$ - lower curve.

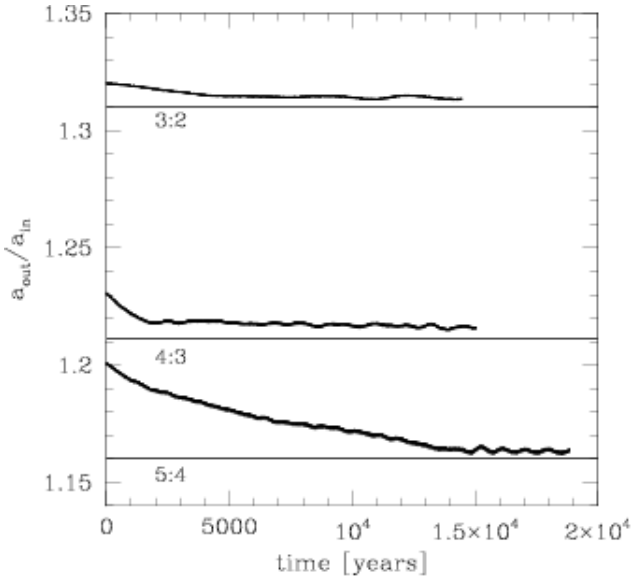

Figure 12. The semi-major axis ratio when $m_1 = m_2 = 4M_\oplus$ with $\Sigma_0 = \Sigma_1$ (uppermost curve) and with $\Sigma_0 = \Sigma_4$ (two lower curves)

When $\Sigma_0 = \Sigma_{0.5}$ the planets enter 4:3 commensurability at a time around 6000 years. The eccentricities of both planets grow. The resonant angle oscillates around 260° with large amplitude, higher than it was in the case when the initial planet separation was smaller, namely 1.2 (Figure 6).
For the disc with the surface density $\Sigma_0 = \Sigma_1$ we can follow in detail the passage of the planets through the 4:3 resonance and the temporary trapping in the 5:4 resonance. In Figure 11 at time 4000 years there is a characteristic rapid increase in the eccentricities of both planets followed by a slower decrease. The angle between the apsidal lines also shows the expected behaviour during resonance crossing. This evolution should be compared with that shown in Figure 5, for the same pair of planets embedded in the same disc but starting with a smaller initial planet separation. The effect of a prior resonance passage before approaching and becoming relatively stably trapped in the 5:4 resonance is not present in this case. So it is likely that the mutual interaction of planets during resonance crossing influences their subsequent evolution and whether higher p resonances are attained or not and that these planets are either close to or in the chaotic regime. This behaviour may be related to the fact that eccentricities excited during resonance passages do not completely decay between them.

3.5 Slower relative migration - planets with equal masses

As described above, the resonant interaction must balance the tendency towards relative migration of the two planets. This is smaller when the planets have the same mass. Thus lower p commensurabilities and less tendency to be driven into a chaotic state might be expected in this case when compared to the situation where the inner planet has significantly smaller mass. In order to investigate this, two planets of mass $4M_\oplus$ were initiated close to 3:2 resonance with $a_1 = 1.32$ and $a_2 = 1$ in a disc with $\Sigma_0 = \Sigma_1$. The evolution of the semi-major axis ratio for the planet orbits is shown in Figure 12. We also performed simulations for the same masses starting with $a_1 = 1.23$ and $a_2 = 1.00$ in a disc with $\Sigma_0 = \Sigma_4$ and $a_1 = 1.2$ and $a_2 = 1$ in a disc with $\Sigma_0 = \Sigma_4$. The planets become trapped in the nearest available resonance which is a good indication of stability. The evolution of the equal mass pair of planets is shown in Figures 13-15. The planets attaining 3:2 resonance after around 4000 years show the following behaviour. Their eccentricities increased until at 8000 years $e_1 = 0.013$ and $e_2 = 0.007$. They then start to oscillate. At around time 13000 the inner planet eccentricity dropped to zero for short period of time. The resonant angle oscillates around 200°.
The planets placed close to 4:3 resonance become locked in this resonance at around 2000 years. The eccentricities of both planets change in a similar way. They do not grow much, towards the end of the simulation they oscillate around 0.008. The angle between apsidal lines and the resonant angle oscillate around 180° and 230°, respectively. The last experiment of this series was as follows. The two planets are initially located just interior to 4:3 resonance. After 12000 years they arrive through convergent migration at the 5:4 resonance and become trapped in it. The eccentricities of the two planets evolve together in an oscillatory way. At time around 16000 years they are very close to zero. Particular features at that time are seen in the evolution of the angle between apsidal lines as well as the resonant angle which are not properly defined for zero eccentricity.

We also performed calculations with two planets of 30 $M_\oplus$ starting with $a_1 = 1.3$ and $a_2 = 1$. The planets were embedded in a disc with $\Sigma_0 = \Sigma_1$. They attained a stable 3:2 resonance. The behaviour of the ratio of semi-major axes close to the resonance is shown in Figure 16 and other aspects of the evolution are shown in Figure 17. The excursions around resonance are lager and noisier in this case. Note too

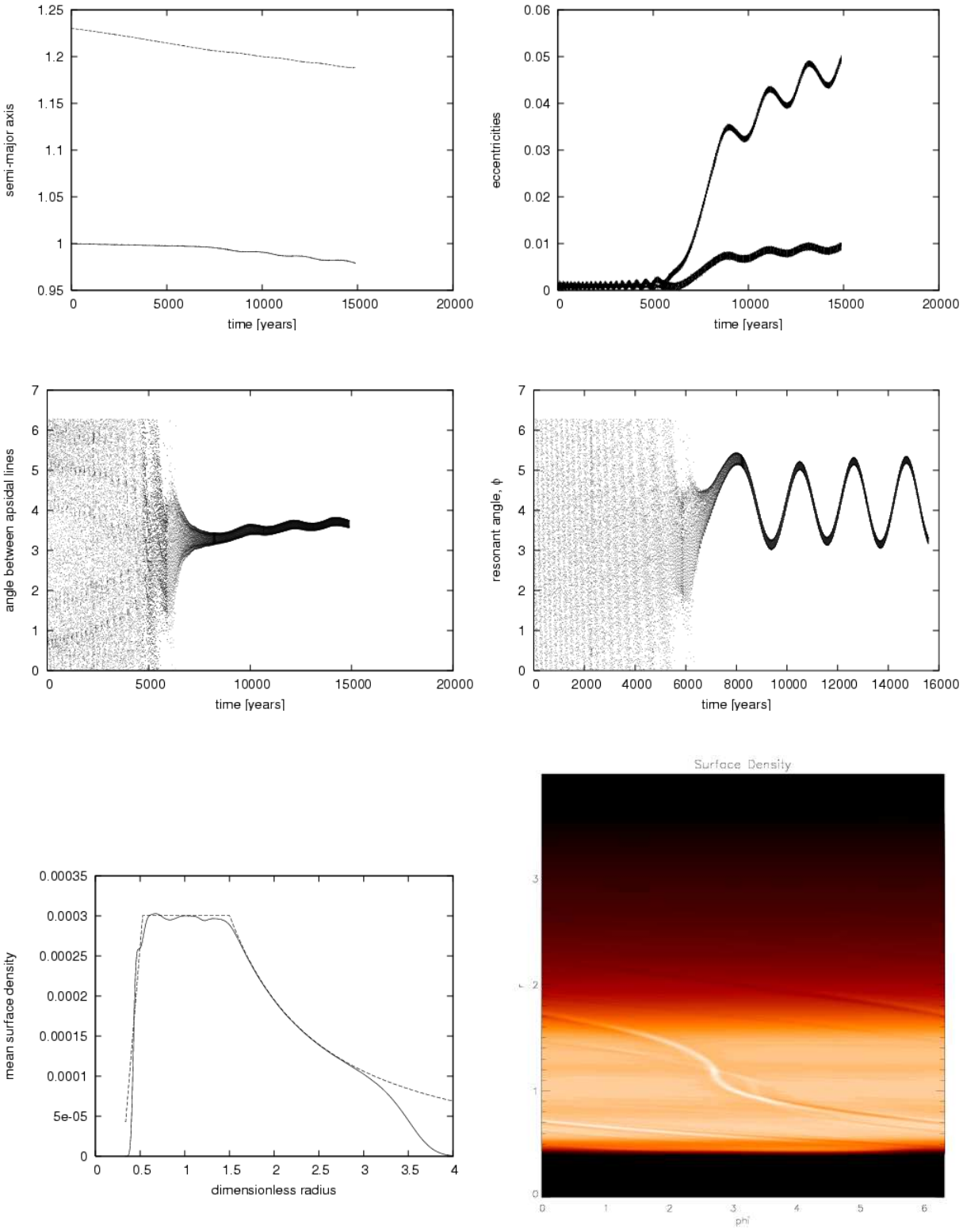

Figure 10. As for Figure 6 but here the planets initially have $a_1/a_2 = 1.23$.

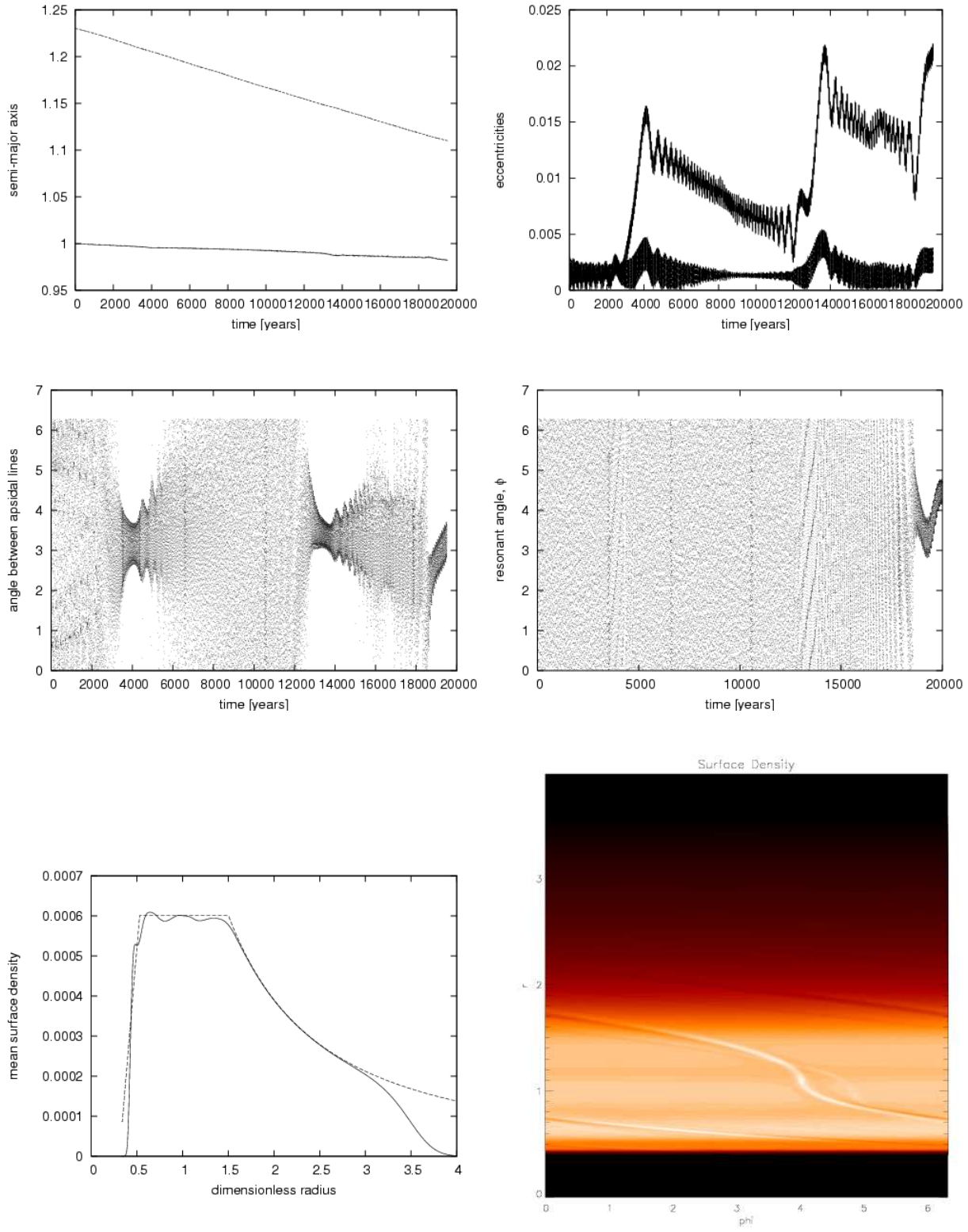

Figure 11. As for Figure 5 but when the planets are initiated with $a_1/a_2 = 1.23$. Note that the system fails to become trapped in the 4:3 and 5:4 commensurabilities but nonetheless shows associated strong resonant interaction for long periods of time around $t = 4000$ and $t = 14000$ years respectively.

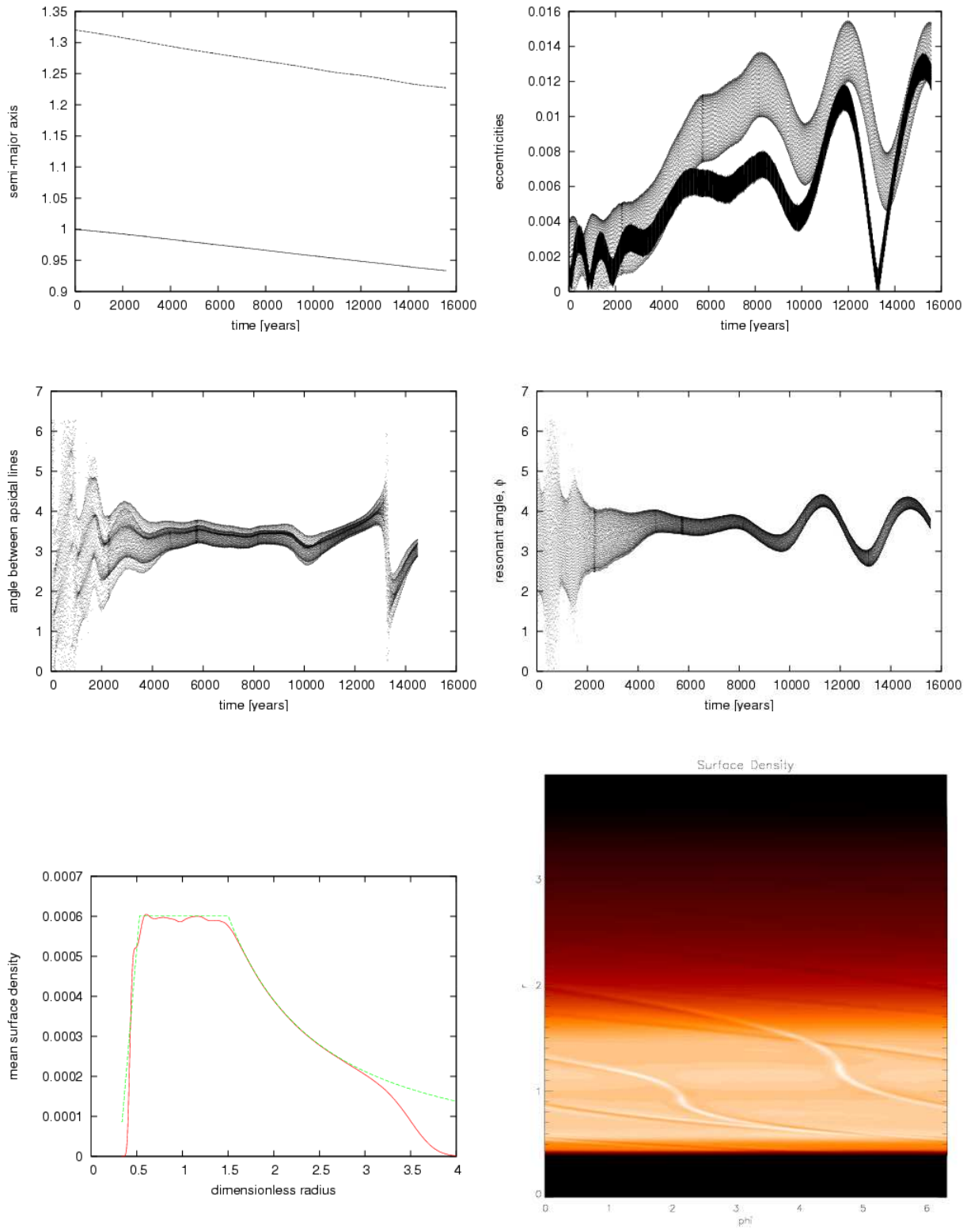

Figure 13. The evolution of semi-major axes, eccentricities, angle between apsidal lines and resonant angle for two planets with equal mass, $m_1 = m_2 = 4M_\oplus$, migrating towards a central star and embedded in a disc with $\Sigma_0 = \Sigma_1$. (four upper panels). The mean surface density profile of the disc near the end of the simulations (solid line), together with the initial surface density profile (dashed line) and a surface density contour plot near the end of the simulation are given in the lowest left and right panels respectively.

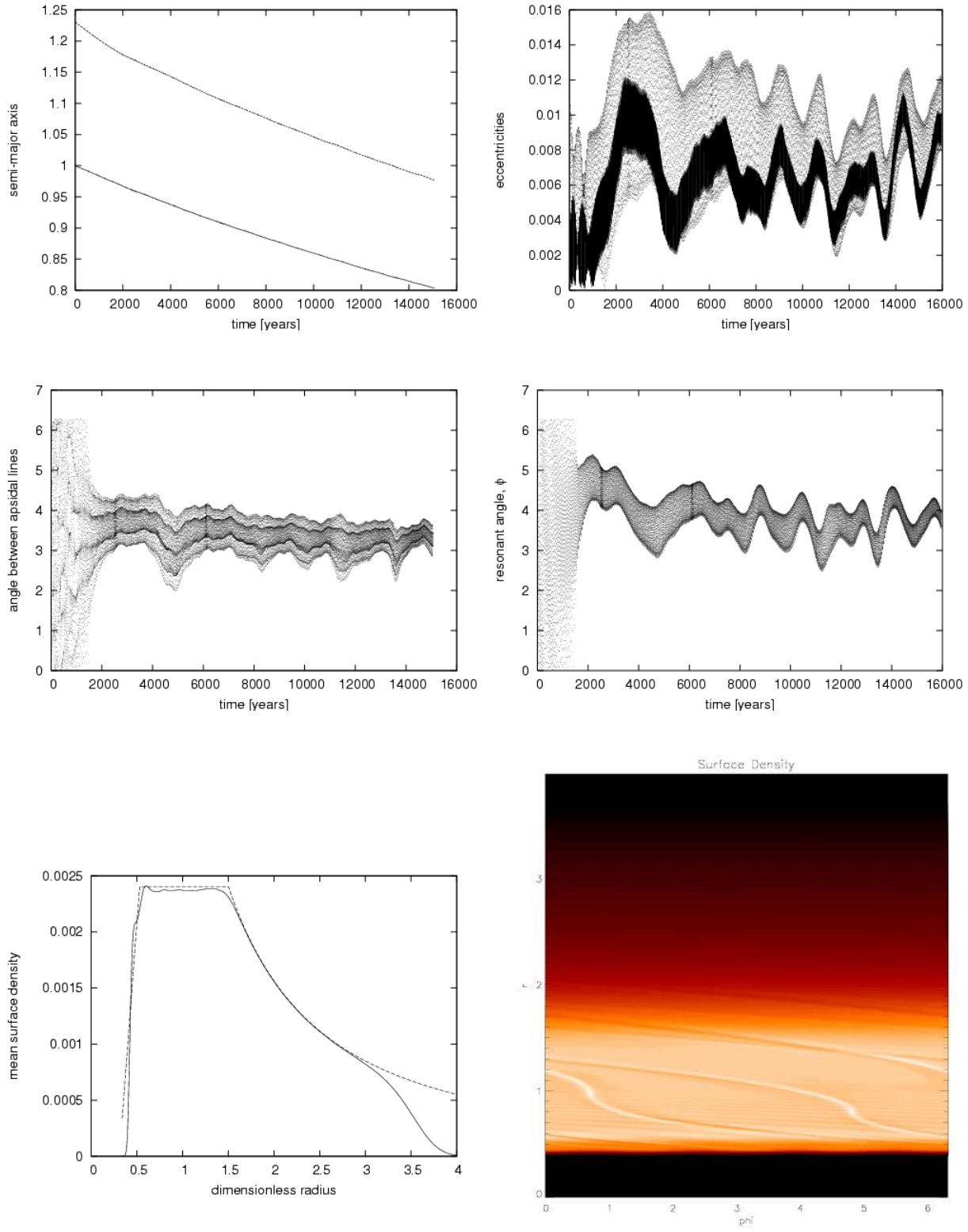

Figure 14. The same as for Figure 13 but the planets initially had $a_1 = 1.23$ and $a_2 = 1$ and they are embedded in a disc with $\Sigma_0 = \Sigma_4$

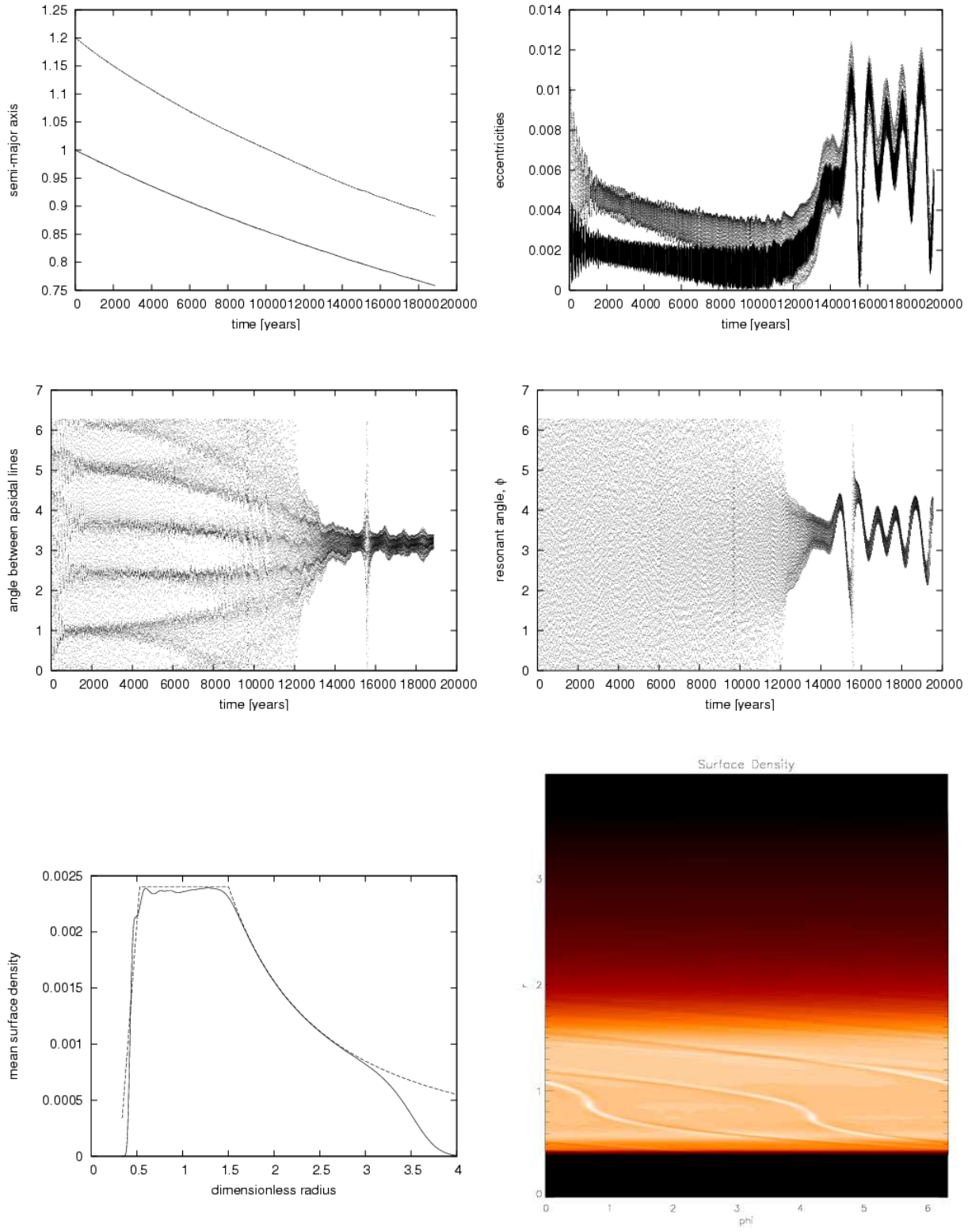

Figure 15. The same as for Figure 13 but the planets initial separation ratio is 1.2 and they are embedded in the disc with $\Sigma = \Sigma_4$

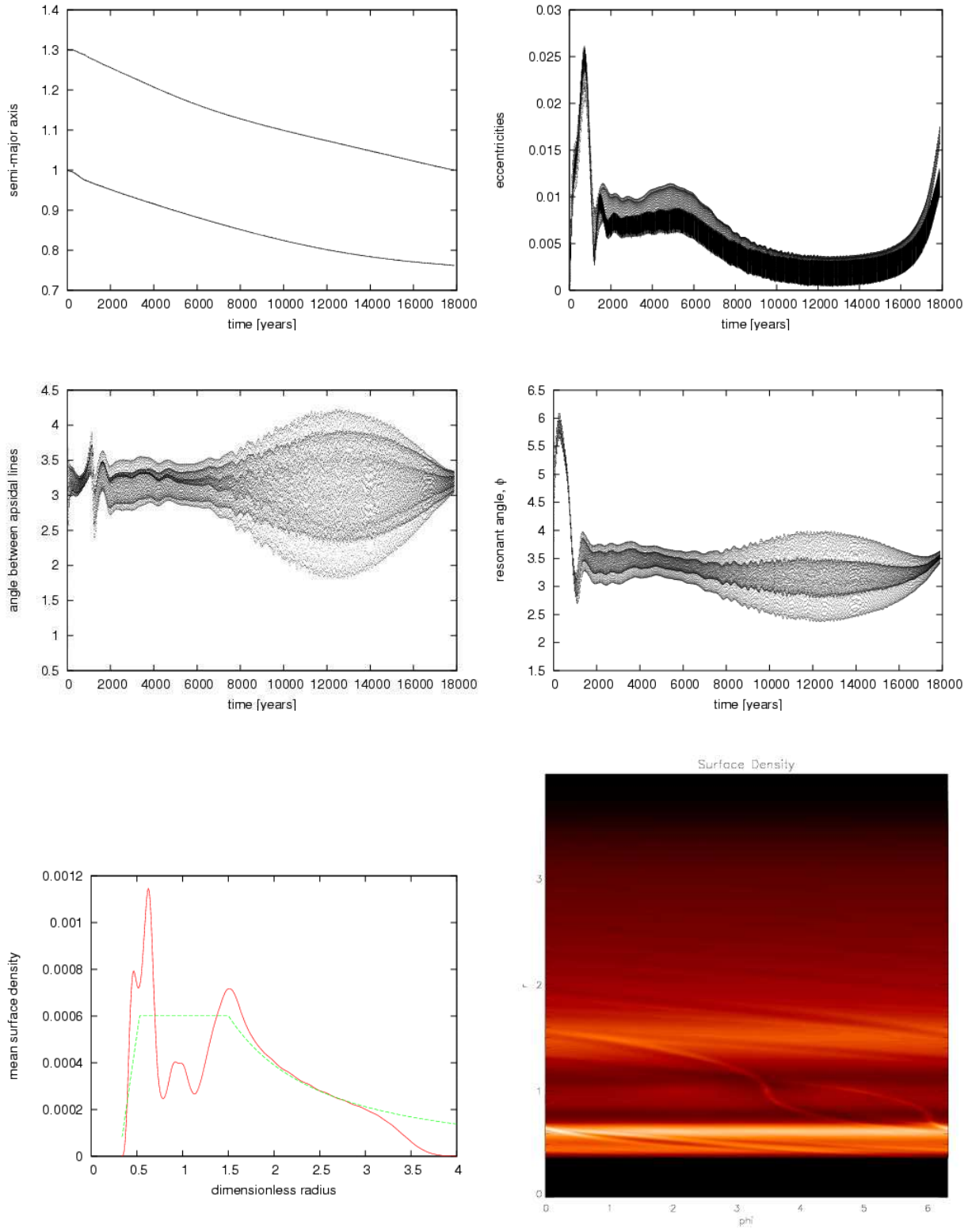

Figure 17. The evolution of semi-major axes, eccentricities, angle between apsidal lines and resonant angle for two planets with masses, $m_1 = 30M_\oplus$ and $m_2 = 30M_\oplus$ migrating towards a central star embedded in a disc with $\Sigma_0 = \Sigma_1$ (four upper panels). The mean surface density profile of the disc near the end of the simulation (solid line) together with the initial surface density profile (dashed line) and a surface density contour plot near the end of the simulation are given in lowest left and right panels respectively.

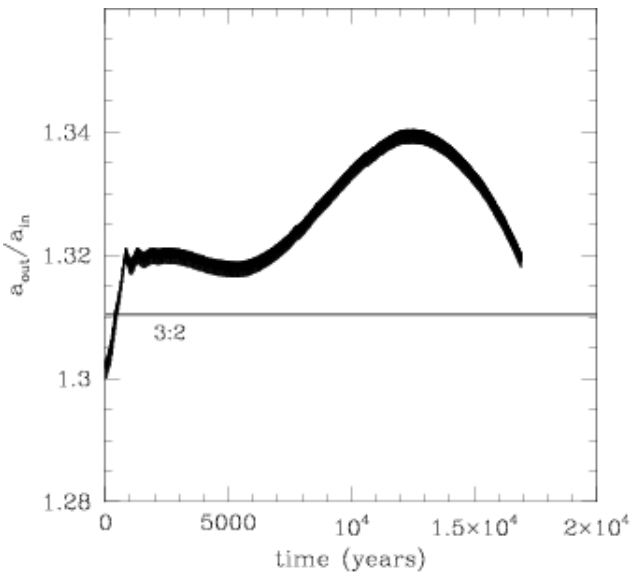

Figure 16. The ratio of semi-major axes for two equal mass planets of $30M_\oplus$, and disc surface density scaling $\Sigma_0 = \Sigma_1$.

that in this case the disc planet interaction becomes non linear with significant perturbation to the underlying disc surface density. There is a tendency towards gap formation and the excavation of disc material into two mounds at the gap edges. The inner mound occupies only a small radial region and so may not be well represented with the available numerical resolution in this case.

4 N-BODY INVESTIGATIONS - A SURVEY

In order to study migrating planets with a wider range of masses and disc surface densities, we have performed a resonance survey using an N-body code. The approach is the same as that used by Snellgrove, Papaloizou & Nelson (2001) and Nelson & Papaloizou (2002) and it has also been used by Lee & Peale (2002) and Kley, Peitz & Bryden (2004). The reader is referred to those papers for details. The procedure is to model the effects of a disc by incorporating orbital migration and eccentricity damping as described by equations (1 - 2) through the addition of appropriate acceleration terms to the equations of motion. We summarize the parameters and outcomes of some of the N body simulations in Table 1.

We begin by discussing a calibration procedure which enables a matching of the N body simulations with the hydrodynamic simulations. The advantage of the N body simulations is that the time evolution of a system can be followed for a much longer period of time. After discussing a few examples, we move on to discuss the results, shown in Table 1, on the possible commensurabilities to be expected for low mass planets for particular choices of their masses, disc parameters and migration and eccentricity damping rates.

4.1 Comparison between hydrodynamic simulations and N-body calculations

The hydrodynamical calculations discussed in the previous Section allow us to follow planets migrations for almost 2×10^4 years. As a result of this we have been able to simulate planets becoming trapped in resonances. The behaviour and stability of the resonance trapping varies with the planet masses and the surface density of the disc in which they are embedded. The outcome of these simulations could be well matched to those of N-body integrations where we incorporate the simple prescriptions for the migration and eccentricity damping given through equations (1-2).

Using these expressions in the N-body code we have extended the hydrodynamic calculations for a longer period of time and studied the long term stability of the resonances we have found in that context. As a first step we have adjusted the numerical coefficients in equations (1-2) in such a way that the hydrodynamic and N-body approach give the same qualitative evolution.

As an example in Figure 18 we show the results of the comparison for the case of two planets with masses 1 $M_\oplus$ and 4 $M_\oplus$ respectively embedded in a disc with initial surface density scaling parameter $\Sigma_0 = \Sigma_4$. The numerical coefficients adopted were $W_m = 0.3647$ and $W_c = 0.225$. These results show good agreement with the hydrodynamic results (see Figure 3) and display the same 8:7 commensurability. The fitted coefficients were also reasonably close to those expected from the analytic disc planet interaction theory, confirming both the migration and eccentricity damping times. Though the latter were typically $\sim$ 40% longer than expected from the analytic theory. The evolution was followed using the N-body approach for an additional 1.2×10^6 years. The two planets remain in the 8:7 resonance during this time and there is no indication of any significant changes in the monitored quantities for the last 9×10^5 years. The long term evolution of this system is shown in Figure 19. It is interesting to note that the equilibrium value of eccentricity of the inner planet is around $e_2 = 0.03$, in accordance with the value predicted by the simple analytic model discussed in Section 2 and derived in the Appendix. The angle between apsidal lines is close to 180° the other resonant angles occupy a wide band between 80° and 287°. A similar procedure has been applied to other cases presented in Section 3. The values of the numerical coefficients (W_m, W_c) used in equations (1-2) obtained by comparing and matching the planet evolution calculated by hydrodynamic and N-body codes are given in Table 2.

In the case of two planets with masses, $m_1 = 4M_\oplus$ and $m_2 = 1M_\oplus$ migrating towards a central star embedded in the disc with $\Sigma_0 = \Sigma_2$ the situation is less stable. The 7:6 resonance found in the hydrodynamic simulations is maintained for around 2×10^5 years, later there is a shift into a 10:9 commensurability. Finally at around 6×10^5 years scattering occurred. Also the 5:4 commensurability in the lower surface density case ($\Sigma_0 = \Sigma_1$) was maintained only until 1.2×10^5 years, then there is a transition to 6:5 which lasted till 2.1×10^5 years. Next, the planets evolved till 6×10^5 years locked in 7:6 resonance and after that continued in 8:7. That was the status of the evolution at the end of our calculations at 1.3×10^6 years. The same pair of planets embedded in the disc with even lower surface density ($\Sigma_0 = \Sigma_{0.5}$) mi-

Table 1. This table lists some of N body calculations of interacting planets with imposed migration and eccentricity damping rates, assumed to result from interaction with a disc, that we performed, together with their outcomes. During these calculations the migration has been followed for a period of time in which the inner planet changes its semi-major axis from $a_2 = 1$ to $a_2 = 0.385$ in dimensionless units. The outer planet is initially placed in circular orbit at $r = 1.4$ in dimensionless units. Thus the situation corresponds with appropriate scaling to the inner planet being initiated at 5.2AU and then migrating to 2AU. Column 1 gives the planet mass ratio, columns 2 and 3 give the outer and inner planet mass in Earth masses respectively. Columns 4-7 indicate the outcome of the interaction as either attainment of a commensurability or a scattering for those cases where the migration was too rapid for that to occur. Where there is a scattering, the radius where it occurred is indicated in dimensionless units in brackets. An asterisk indicates that the resonance showed signs of instability that would result in the transition to a higher p resonance on further inward migration which could not be followed.

m_1/m_2	m_1	m_2	$\Sigma_0 = \Sigma_{0.5}$	$\Sigma_0 = \Sigma_1$	$\Sigma_0 = \Sigma_2$	$\Sigma_0 = \Sigma_4$
100/3	100/3	1	5:4*	scatter(0.77)	5:4	scatter(0.87)
20	20	1	4:3*	scatter(0.57)	6:5	scatter(0.96)
10	10	1	7:6*	8:7*	scatter(0.87)	scatter(0.38)
10	100/3	10/3	no resonance	6:5	scatter(0.67)	scatter(0.67)
25/3	100/3	4	6:5	scatter(0.67)	5:4*	scatter(0.88)
6	20	10/3	5:4*	6:5*	6:5	7:6
5	20	4	5:4	7:6	6:5	7:6
4	4	1	6:5	6:5*	7:6	10:9*
10/3	10/3	1	5:4	6:5*	8:7	9:8*
10/3	100/3	10	4:3	4:3	5:4	6:5
3	10	10/3	4:3	5:4	6:5	7:6
5/2	10	4	4:3	4:3	5:4	6:5
2	20	10	3:2	3:2	4:3	5:4
5/3	100/3	20	3:2	3:2	4:3	5:4
6/5	4	10/3	3:2	3:2	3:2	4:3
1	1	1	3:2	3:2	3:2	3:2
1	10/3	10/3	3:2	3:2	3:2	3:2
1	4	4	3:2	3:2	3:2	3:2
1	10	10	3:2	3:2	3:2	3:2
1	20	20	3:2	3:2	3:2	3:2
1	100/3	100/3	3:2	3:2	3:2	3:2

Table 2. The fitting parameters obtained by comparing hydrodynamic and N-body calculations

r_1/r_2	m_1/m_2	Σ_0	W_m	W_c
1.2	4	$\Sigma_{0.5}$	0.3134	0.140
1.2	4	Σ_1	0.3419	0.175
1.2	4	Σ_2	0.3611	0.175
1.2	4	Σ_4	0.3647	0.225
1.2	1	$\Sigma_{0.5}$	0.3277	0.080
1.2	1	Σ_4	0.3706	0.080
1.32	4	$\Sigma_{0.5}$	0.3134	0.190
1.32	4	Σ_4	0.3604	0.210
1.32	1	Σ_1	0.3619	0.200
1.23	4	$\Sigma_{0.5}$	0.3277	0.170
1.23	4	Σ_1	0.3131	0.190
1.23	1	$\Sigma_{0.5}$	0.3419	0.200
1.23	1	Σ_4	0.4274	0.200

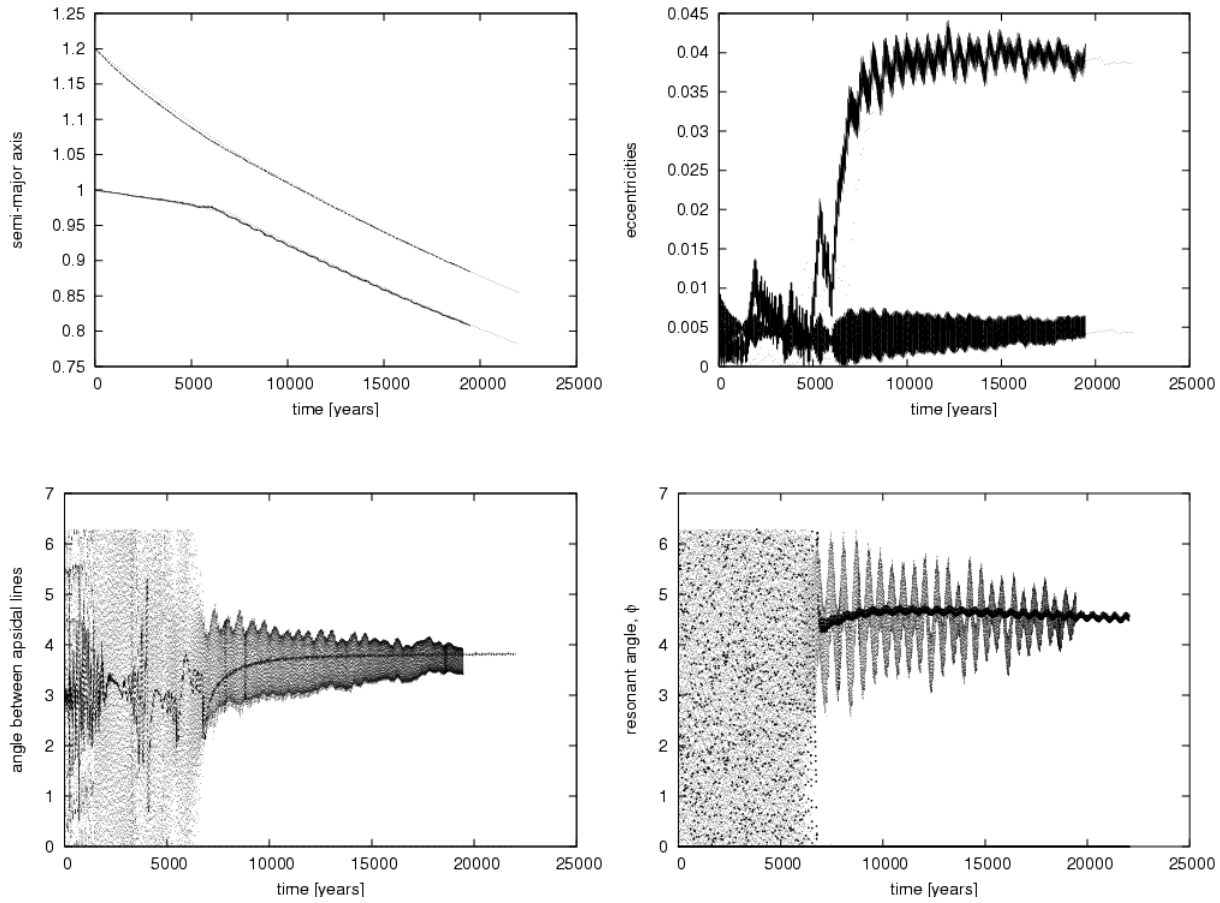

Figure 18. The evolution of semi-major axes, eccentricities, angle between apsidal lines and resonant angle for two planets with masses, $m_1 = 4M_\oplus$ and $m_2 = 1M_\oplus$ migrating towards a central star embedded in the disc with $\Sigma = \Sigma_4$ obtained by N-body simulation (dotted lines in two upper panels and dark lines in two lower panels) superimposed onto the hydrodynamic simulation shown already in Figure 3.

grated together in 5:4 resonance till 1.15×10^6 years, then they moved into a 6:5 commensurability. These outcomes are suggestive of the long term instability of the high p commensurabilities (Kary, Lissauer & Greenzweig 1993).

We have noticed a strong sensitivity of outcomes to the fitting parameters (especially in the numerical coefficient W_m. This is symptomatic of chaotic motion. A very small change in the values of the numerical coefficients given in Table 2 can produced large variations in outcomes. The value W_c is difficult to fit for pairs of two equal mass planets because of smaller and less regular changes in eccentricities obtained in the hydrodynamic simulations of such systems (see for example Figure 13).

4.2 N-body resonance survey

We applied the much faster N-body calculations to extend our hydrodynamic simulations to a wider range of planet masses and disc surface densities. The results are summarized in Table 1. We allowed the numerical coefficients W_m and W_c in equations (1-2), when used in the N body evolution, to be free parameters that we could choose to provide the best match between the hydrodynamic and N body methods. In this way we could test the applicability of the results of Tanaka, Takeuchi & Ward (2002) and Tanaka & Ward (2004) to this problem.

When we chose $W_m = 0.3704$ in equation (1) and $W_c = 0.289$ in equation (2) for the case when the planets have equal masses, $(m_1/m_2) = 1$, their initial separation in circular orbits in dimensionless units is such that $r_1/r_2 = 1.4$ and they are embedded in a disc which extends from $r = 0.3$ to $r = 1.4$, than the most likely outcome of their orbital evolution caused by the disc-planet interaction, in agreement with the hydrodynamic simulations, is attainment of a 3:2 commensurability. This is the case for a wide range of disc surface density scalings. For all values of Σ_0 considered here, this commensurability was attained. A transition from the 3:2 commensurability to the 4:3 commensurability for a given mass ratio (bigger than 1) is expected to occur when either the surface density scaling and/or the mass ratio is

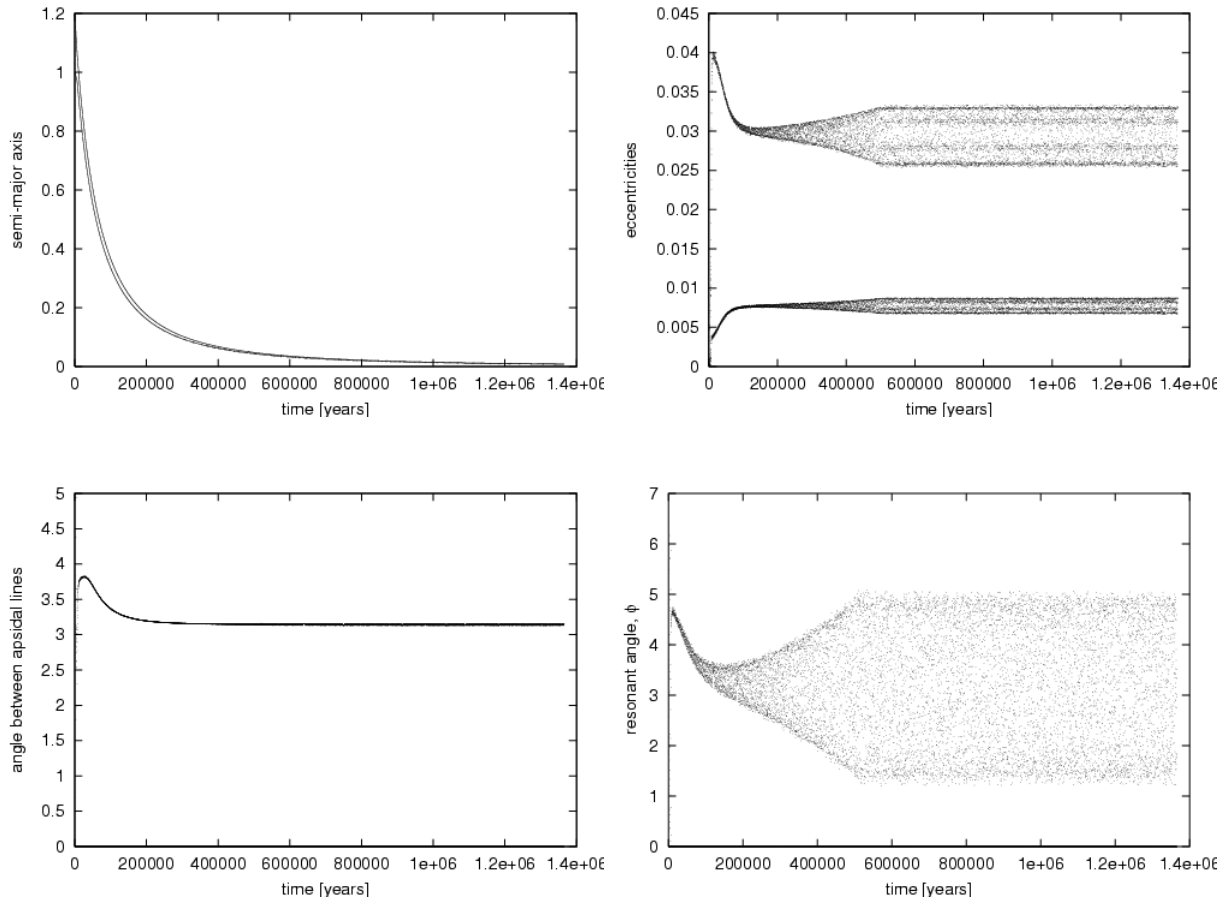

Figure 19. The evolution of the semi-major axes, eccentricities, angle between apsidal lines and resonant angle for two planets with masses, $m_1 = 4M_\oplus$ and $m_2 = 1M_\oplus$ migrating towards a central star embedded in the disc with $\Sigma = \Sigma_4$ obtained with N-body simulations.

large enough. The value of p for the resonance which might be established accordingly increases.

When $m_1/m_2 > 6$ scattering is likely to occur rather than stable resonance trapping, especially for higher surface densities. This is clearly indicated in Table 1.

5 CONCLUSIONS

We have investigated migration induced resonant capture in a system of two planets for the most part in the mass range $1 - 4M_\oplus$ embedded in a gaseous disc. We also considered a system with equal masses of $30M_\oplus$. As the disc was laminar, apart from in the $30M_\oplus$ case, the planets underwent type I migration which occurs through the linear response of the disc to perturbation by the planets. We considered disc surface densities in the range $0.5 - 4$ times that expected for the minimum mass solar nebula at 5.2 AU. Thus migration rates should thus be typical of those expected for standard protoplanetary discs.

Our conclusions are based on the results of two surveys in which we studied the evolution of a pair of planets with a range of planetary masses (1 - $30M_\oplus$), disc surface densities and initial planet separations. The smaller survey used hydrodynamic simulations and because of computational requirements was limited to run lengths of $\sim 2 \times 10^4$ inner planet orbits. Similarly initial conditions which started with the planets too far apart were precluded. A more extensive survey used a simplified N-body approach where the influence of the disc was modelled through the addition of external torques and eccentricity damping terms (see equations (1) and (2)).

The numerical calculations are supplemented with an analytic model describing two planets migrating in resonance with arbitrary eccentricities. We found a very good agreement between numerical and analytical results for an established commensurability.

Both our hydrodynamic and N-body approaches give clear evidence of an interesting relation between the mass ratio in a planetary pair and the type of the resonance which is expected to be established as a consequence of tidally induced orbital migration. When both planets have similar masses, provided the disc surface density at their locations is very

similar, the rate of convergent or relative migration is small. This favours attainment of low p commensurabilities. An example of this occurred in the equal $4M_\oplus$ case we considered. There, the planets became locked in the nearest first order commensurability lying between them. Thus if they were assembled with $1.55 > r_1/r_2 > 1.31$ the migration led to trapping in 3:2 resonance.

Here, we comment that the very well known example of such a system, namely the two largest mass planets orbiting a millisecond radio pulsar PSR B1257+12, are close to a 3:2 commensurability. The most recent determination of the masses of these planets gives them as $4.3 \pm 0.2 M_\oplus$ and $3.9 \pm 0.2 M_\oplus$ respectively, (Konacki & Wolszczan 2003). The mass ratio is thus very close to unity and according to our findings if migration in a standard quiescent protoplanetary gaseous disc is responsible for the evolution then a possible outcome could be attainment of a 3:2 commensurability. The orbital periods for both planets are 66.5419 days and 98.2114 days (Konacki & Wolszczan 2003) which places them near 3:2 resonance. Such a resonance could be formed and maintained through the processes discussed in this paper, with the planets later moving slightly out of resonance. More specific detailed modeling will be presented elsewhere.

For more disparate mass ratios, our simulations indicate the attainment of first order commensurabilities with higher p (for example 4:3, 5:4, 7:6 and 8:7). The dynamics develops a stochastic character, and these may be maintained for a different periods of time before becoming unstable. Then often a passage from one resonance to another takes place. The short duration of the hydrodynamic simulations precluded extensive exploration of stochastic behaviour or the long term stability of resonances. However, we could investigate these issues employing the simplified N-body approach. In this context we comment on a result we have obtained for an 8:7 commensurability, being the stable end state of the evolution of two planets in circular orbit with the initial separation ratio $r_1/r_2 = 1.2$, and mass ratio $m_1/m_2 = 4$ and the highest disc surface density scaling considered here with $\Sigma_0 = \Sigma_4$. The stable configuration was maintained until 1.4×10^6 orbits at which point our calculations were stopped. Of course this result should be considered in the context of extreme sensitivity to initial conditions and other parameters. Nonetheless, the final value of the inner planet eccentricity is in good agreement with the prediction of our analytic model for established commensurabilities.

Thus while stochastic behaviour tends to disrupt higher p commensurabilities, the calculations presented here do not enable us to rule them out entirely.

Simple N-body calculations allowed us to extend our investigations not only to consider longer term behaviour but also a wider range of initial conditions. These calculations strengthen the conclusions derived from the hydrodynamic simulations.

Finally, we comment further on the onset of stochastic behaviour which we encountered both in our hydrodynamic simulations and N-body calculations. The reason for this phenomenon can be related to resonance overlap. According to our estimates we might expect isolated resonances in which a system of planets in the mass range considered can be locked and migrate together to be such that the integer p in the expression $p + 1 : p$ for a first order commensurability is $\lesssim 8$. For larger p, as we can see from Table 1 a system is likely to undergo a scattering and exchange of orbits of the two planets. However, stochastic behaviour may extend to values as small as 4. Stable commensurabilities with sufficiently small p correspond to physically possible planetary configurations and they should be the centre of further investigation.

Among all planned future space missions COROT will be the first with the capability to observe planets in the mass range relevant to our investigation. Studies of commensurabilities have already been applied successfully to analyse the motion of the pulsar planets, and they proved to be a powerful tool in that context. They have the potential to be similarly useful in our search for Earth-like planets in other systems. Detection of such resonances can also yield useful information about orbital migration as a process operating during planet formation.

ACKNOWLEDGMENTS

E.S. would like to express her gratitude for support through its PPARC funded visitors grant and for the provision of computer facilities to the Astronomy Unit, Queen Mary, University of London. E.S. acknowledges the hospitality of the Kavli Institute for Theoretical Physics, University of California, Santa Barbara. This research was supported in part by the National Science Foundation under Grant No. PHY99-0794.

APPENDIX

A simple model

The equations of motion for a system consisting of 2 planets and primary star, modeled as point masses moving under their mutual gravitational attraction, are conveniently expressed in Hamiltonian form using Jacobi coordinates (see Sinclair (1975)). Then the radius vector $\mathbf{r}_2$, of the inner planet of reduced mass m_2 is measured from the primary star of mass M_* and that of the outer planet, $\mathbf{r}_1$, of reduced mass m_1 is referred to the centre of mass of the primary star and inner planet. The Hamiltonian can be written correct to second order in the planetary masses as

$$\begin{aligned} H &= \frac{1}{2}(m_1|\dot{\mathbf{r}}_1|^2 + m_2|\dot{\mathbf{r}}_2|^2) - \frac{GM_{*1}m_1}{|\mathbf{r}_1|} - \frac{GM_{*2}m_2}{|\mathbf{r}_2|} \\ &- \frac{Gm_1m_2}{|\mathbf{r}_{12}|} + \frac{Gm_1m_2\mathbf{r}_1\cdot\mathbf{r}_2}{|\mathbf{r}_1|^3}. \end{aligned} \quad (9)$$

Here $M_{*1} = M_* + m_1, M_{*2} = M_* + m_2$ and $\mathbf{r}_{12} = \mathbf{r}_2 - \mathbf{r}_1$. The Hamiltonian can be expressed in terms of the osculating semi-major axes, eccentricities and longitudes of periastron $a_i, e_i, \varpi_i, i = 1, 2$ respectively as well as the longitudes λ_i, and the time t. We recall that $\lambda_i = n_i(t - t_{0i}) + \varpi_i$, with $n_i = \sqrt{GM_{*i}/a_i^3}$ being the mean motion and t_{0i} giving the time of periastron passage. The energy is given by $E_i = -Gm_iM_{*i}/(2a_i)$, and the angular momentum $h_i = m_i\sqrt{GM_{*i}a_i(1-e_i^2)}$ which may be used to describe the motion instead of a_i and e_i.

The Hamiltonian may quite generally be expanded in a Fourier series involving linear combinations of the three angular differences $\lambda_i - \varpi_i, i = 1, 2$ and $\varpi_1 - \varpi_2$ (eg. Brouwer & Clemence (1961)).

Near a first order $p+1:p$ resonance, we expect that both $\phi=(p+1)\lambda_1-p\lambda_2-\varpi_1$, and $\psi=(p+1)\lambda_1-p\lambda_2-\varpi_2$, will be slowly varying. When resonances are non overlapping so that the $p+1:p$ resonance may be isolated, in its neighborhood, terms in the Fourier expansion involving only linear combinations of ϕ and ψ as argument are expected to produce the largest perturbations, while the remainder, which will have rapidly varying argument, may be averaged out.
The resulting Hamiltonian ($\propto m_1m_2$) may then be written in the general form

$$H_{12}=-\frac{Gm_1m_2}{a_1}\sum C_{k,l}(a_1/a_2,e_1,e_2)\cos(k\phi+l\psi), \quad (10)$$

where in the above and similar summations below, the sum ranges over all positive and negative integers (k,l) and the dimensionless coefficients $C_{k,l}$ depend on e_1,e_2 and the ratio a_1/a_2 only. Here we shall not need to specify these further. We also make the inconsequential simplification of replacing M_{*i} by M_*.

Basic Equations

We take the Hamiltonian system derived from (10) and modify it by incorporating torques and rates of change of energy that act on each of the protoplanets and which are presumed to be derived from interaction with the disc.

The equations of motion are very similar to those given in Papaloizou (2003). They differ only in that the additional forces derived from disc interaction are allowed to act on both protoplanets rather than only the outer one in this case.
$dE_i/dt=-n_i\partial H_{12}/\partial\lambda_i-(n_iT_i/\sqrt{1-e_i^2}+D_i)$,
$dh_i/dt=-\partial H_{12}/\partial\lambda_i-\partial H_{12}/\partial\varpi_i-T_i$,
$d\lambda_i/dt=n_i+n_i\partial H_{12}/\partial E_i+\partial H_{12}/\partial h_i$,
$d\varpi_i/dt=\partial H_{12}/\partial h_i$,

The external disc torque acting on the planet m_i is $-T_i$. Associated with this, we remove orbital energy at a rate $n_iT_i/\sqrt{1-e_i^2}$ from m_i which would correspond to the action of a disc density perturbation rotating with a pattern speed $n_i/\sqrt{1-e_i^2}$ (see also Snellgrove, Papaloizou & Nelson (2001); Nelson & Papaloizou (2002)). We include an additional energy loss rate D_i for m_i which leads to an orbital circularization time for m_i given by

$$t_{ci}=\frac{n_im_ie_i^2\sqrt{GM_*a_i}}{D_i(1-e_i^2)}. \quad (11)$$

This circularization time is such that if the the other planet was absent such that m_i was affected only by the central star and disc, e_i would decay according to

$$\frac{de_i}{dt}=\frac{-e_i}{t_{ci}}. \quad (12)$$

We presume that T_i, and D_i are given as functions of the orbital parameters a_i,e_i associated with m_i. In addition we suppose that they lead to orbital evolution on a timescale sufficiently long compared to other effects that they may always be considered to act as small perturbations to the equations of motion. However, we do not assume an expansion in terms of small eccentricities.

We thus obtain to lowest order in the perturbing masses.

$$\frac{dn_1}{dt} = \frac{3(p+1)n_1^2m_2}{M_*}\sum C_{k,l}(k+l)\sin(k\phi+l\psi) + \frac{3n_1a_1}{GM_*m_1}\left[\frac{n_1T_1}{\sqrt{1-e_1^2}}+D_1\right] \quad (13)$$

$$\frac{dn_2}{dt} = -\frac{3pn_2^2m_1a_2}{M_*a_1}\sum C_{k,l}(k+l)\sin(k\phi+l\psi) + \frac{3n_2a_2}{GM_*m_2}\left[\frac{n_2T_2}{\sqrt{1-e_2^2}}+D_2\right] \quad (14)$$

$$\frac{de_1}{dt}=-\frac{e_1}{t_{c1}}-\frac{m_2n_1\sqrt{1-e_1^2}}{e_1M_*}\times \sum C_{k,l}\sin(k\phi+l\psi)\left(k-(p+1)(k+l)(1-\sqrt{1-e_1^2})\right) \quad (15)$$

$$\frac{de_2}{dt}=-\frac{e_2}{t_{c2}}-\frac{m_1a_2n_2\sqrt{1-e_2^2}}{a_1e_2M_*}\times \sum C_{k,l}\sin(k\phi+l\psi)\left(l+p(k+l)(1-\sqrt{1-e_2^2})\right) \quad (16)$$

$$\frac{d\phi}{dt}=(p+1)n_1-pn_2-\sum(D_{k,l}+E_{k,l})\cos(k\phi+l\psi). \quad (17)$$

$$\frac{d\psi}{dt}=(p+1)n_1-pn_2-\sum(D_{k,l}+F_{k,l})\cos(k\phi+l\psi). \quad (18)$$

Here

$$D_{k,l} = \frac{2(p+1)n_1a_1^2m_2}{M_*}\frac{\partial}{\partial a_1}\left(C_{k,l}/a_1\right) - \frac{2pn_2a_2^2m_1}{M_*}\frac{\partial}{\partial a_2}\left(C_{k,l}/a_1\right), \quad (19)$$

$$E_{k,l} = \frac{n_1m_2((p+1)(1-e_1^2)-p\sqrt{1-e_1^2})}{e_1M_*}\frac{\partial C_{k,l}}{\partial e_1} + \frac{pn_2a_2m_1(\sqrt{1-e_2^2}-1+e_2^2)}{a_1e_2M_*}\frac{\partial C_{k,l}}{\partial e_2} \quad (20)$$

and

$$F_{k,l} = \frac{(p+1)n_1m_2(1-e_1^2-\sqrt{1-e_1^2})}{e_1M_*}\frac{\partial C_{k,l}}{\partial e_1} + \frac{n_2a_2m_1((p+1)\sqrt{1-e_2^2}-p(1-e_2^2))}{a_1e_2M_*}\frac{\partial C_{k,l}}{\partial e_2}. \quad (21)$$

We further note that $\phi-\psi=\varpi_2-\varpi_1$ is the angle between the two apsidal lines of the two planetary orbits.

Time Independent Solutions

When no external disc torques or dissipation act ($T_i=D_i=0$) time independent or stationary solutions may occur for which ψ, ϕ and each of n_1,n_2,e_1,e_2 are constant. In principle any stationary values of $\psi=\psi_0$ and $\phi=\phi_0$ might be possible. Obvious possibilities, as also indicated in our numerical simulations, are values of ϕ_0 and ψ_0 that are either 0, or π. In that case it follows directly from equations (13-16) with $T_i=D_i=0$ that there are stationary solutions with n_1,n_2,e_1,e_2 being constant. In other cases, consideration of

equations (13 - 18) indicates that we should regard ϕ_0 and ψ_0 as functions of e_1, e_2 and the ratio a_2/a_1.
A relation between e_1, e_2 and the ratio a_2/a_1 for steady solutions follows by subtracting equations (17) and (18) in the form

$$\sum (E_{k,l}\cos(k\phi_0 + l\psi_0) = \sum F_{k,l}\cos(k\phi_0 + l\psi_0) = S_p. \quad (22)$$

This condition in fact matches the precession rates of the orbits of the two planets such that they maintain a fixed orientation. It then additionally follows from equations (17) and (18) that

$$(p+1)n_1 - pn_2 = \sum D_{k,l}\cos(k\phi_0 + l\psi_0) + S_p. \quad (23)$$

This gives a further relation between e_1, e_2 and the ratio a_2/a_1. We could for example specify e_1 and then both e_2 and a_2/a_1 would be specified but in any case the quantity $((p+1)n_1)/(pn_2) - 1$, supposing m_1 and m_2 to be comparable, is at least of order of smallness of the mass ratio $m_1/M_* \ll 1$. Thus in a perturbation quantity that is already first order in the perturbing masses we may set $a_2/a_1 = ((p+1)/p)^{-2/3}$ which gives the condition for a $p+1:p$ commensurability.

Time Dependent Solutions with Migration and Circularization

We now generalize the above solution to incorporate the effects of small non zero disc torques T_i and dissipation D_i. In this case the two planets migrate inwards locked in resonance with n_1/n_2 maintained nearly equal to $p/(p+1)$. In the absence of any tidal effects which could act to circularize the orbits the eccentricities are found to increase monotonically with time. We note that equations (13-14) define inward migration timescales or e folding rates for n_i as $t_{migi} = GM_* m_i\sqrt{1-e_i^2}/(3T_i a_i n_i)$. We suppose that in order to accommodate small values of T_i and D_i, the angles $\psi_1 = \psi - \psi_0$ and $\phi_1 = \phi - \phi_0$, which measure the departures from the values appropriate to the steady state solution, take on non zero values of small magnitude which can also change very slowly with time. These magnitudes are presumed sufficiently small that we may employ a first order Taylor expansion so that the perturbation to $\sin(k\phi + l\psi)$ is $(k\phi_1 + l\psi_1)\cos(k\phi_0 + l\psi_0)$ and similarly the perturbation to $\cos(k\phi + l\psi)$ is $-(k\phi_1 + l\psi_1)\sin(k\phi_0 + l\psi_0)$.
When the migration time is very long compared to any other time scale in the problem, equations (17) and (18) are of the same form as in the time independent case, apart from small corrections proportional to the migration rate which we neglect. These then lead to the same conclusions as in the time independent case. Accordingly we conclude that there are relationships between e_1, e_2 and a_2/a_1 which specify the latter two once e_1 is specified but that always a_2/a_1 satisfies the condition for $(p+1):p$ resonance with a correction of order of the perturbing masses.

Equations (13-16) then become

$$\frac{dn_1}{dt} = \frac{3(p+1)n_1^2 m_2}{M_*}\sum \mathcal{C}_{k,l}(k+l)(k\phi_1 + l\psi_1) + \frac{3n_1 a_1}{GM_* m_1}\left[\frac{n_1 T_1}{\sqrt{1-e_1^2}} + D_1\right] \quad (24)$$

$$\frac{dn_2}{dt} = -\frac{3pn_2^2 m_1 a_2}{M_* a_1}\sum \mathcal{C}_{k,l}(k+l)(k\phi_1 + l\psi_1) + \frac{3n_2 a_2}{GM_* m_2}\left[\frac{n_2 T_2}{\sqrt{1-e_2^2}} + D_2\right] \quad (25)$$

$$\frac{de_1}{dt} = -\frac{e_1}{t_{c1}} - \frac{m_2 n_1\sqrt{1-e_1^2}}{e_1 M_*} \times \sum \mathcal{C}_{k,l}(k\phi_1 + l\psi_1)\left(k - (p+1)(k+l)(1-\sqrt{1-e_1^2})\right) \quad (26)$$

$$\frac{de_2}{dt} = -\frac{e_2}{t_{c2}} - \frac{m_1 a_2 n_2\sqrt{1-e_2^2}}{a_1 e_2 M_*} \times \sum \mathcal{C}_{k,l}(k\phi_1 + l\psi_1)\left(l + p(k+l)(1-\sqrt{1-e_2^2})\right). \quad (27)$$

Here $\mathcal{C}_{k,l} = C_{k,l}\cos(k\phi_0 + l\psi_0)$.
Taking the ratio of (24) and (25) gives

$$\frac{dn_1}{dn_2} = -\frac{(p+1)n_1^2 m_2 a_1 \sum \mathcal{H}_{k,l}(k+l) + \frac{n_1 a_1^2}{Gm_1}\left(\frac{n_1 T_1}{\sqrt{1-e_1^2}} + D_1\right)}{pn_2^2 m_1 a_2 \sum \mathcal{H}_{k,l}(k+l) - \frac{n_2 a_1 a_2}{Gm_2}\left(\frac{n_2 T_2}{\sqrt{1-e_2^2}} + D_2\right)}, \quad (28)$$

with $\mathcal{H}_{k,l} = \mathcal{C}_{k,l}(k\phi_1 + l\psi_1)$.
The ratio of (26) and (27) gives another relation of the form

$$\frac{m_2 e_2 a_1 n_1\sqrt{1-e_1^2}}{m_1 e_1 a_2 n_2\sqrt{1-e_2^2}}\frac{de_2}{de_1} = \frac{\sum \mathcal{H}_{k,l}(l + p(k+l)(1-\sqrt{1-e_2^2})) + \frac{e_2^2 M_* a_1}{\sqrt{1-e_2^2} m_1 a_2 n_2 t_{c2}}}{\sum \mathcal{H}_{k,l}(k - (p+1)(k+l)(1-\sqrt{1-e_1^2})) + \frac{e_1^2 M_*}{\sqrt{1-e_1^2} m_2 n_1 t_{c1}}}, \quad (29)$$

Using $pn_2 = (p+1)n_1$, equation (28) gives

$$\phi_1 \sum k\mathcal{C}_{k,l}(k+l) + \psi_1 \sum l\mathcal{C}_{k,l}(k+l) = \frac{-(p+1)n_1 a_1^2 m_2\left(\frac{n_1 T_1}{\sqrt{1-e_1^2}} + D_1\right) + pm_1 n_2 a_1 a_2\left(\frac{n_2 T_2}{\sqrt{1-e_2^2}} + D_2\right)}{Gm_1 m_2\left((p+1)^2 n_1^2 m_2 a_1 + p^2 n_2^2 m_1 a_2\right)} \quad (30)$$

Given that we may regard e_2 and a_2/a_1 as functions of e_1, we may also regard equations (28) and (29) as determining ϕ and ψ as functions of a_1, and e_1. Using this information, equations (24) and (26) may be used to determine n_1 and e_1 as functions of time so completing the solution.
One readily finds that these satisfy

$$\frac{1}{n_1}\frac{dn_1}{dt} = 3 \times \frac{m_1 a_2\left(\frac{1}{3t_{mig1}} + \frac{e_1^2}{(1-e_1^2)t_{c1}}\right) + a_1 m_2\left(\frac{1}{3t_{mig2}} + \frac{e_2^2}{(1-e_2^2)t_{c2}}\right)}{[m_2 a_1 + m_1 a_2]} \quad (31)$$

$$e_1\frac{de_1}{dt} = -\frac{e_1^2}{\Lambda t_{c1}} - \frac{e_1 e_2(\Lambda - 1)}{\Lambda t_{c2}}\frac{de_1}{de_2} + \frac{\left(\left(\frac{1}{3t_{mig1}} + \frac{e_1^2}{(1-e_1^2)t_{c1}}\right) - \left(\frac{1}{3t_{mig2}} + \frac{e_2^2}{(1-e_2^2)t_{c2}}\right)\right)\mathcal{T}}{\Lambda\left[m_2 a_1 + m_1 a_2\right]} \quad (32)$$

where

$$\Lambda = 1 + \frac{e_2}{e_1}\frac{de_2}{de_1}\left[\frac{\sqrt{1-e_1^2}m_2n_1a_1}{\sqrt{1-e_2^2}m_1n_2a_2}\right] \quad (33)$$

and

$$\mathcal{T} = \frac{m_2a_1\sqrt{1-e_1^2}}{p+1} \times\left(1-(p+1)(1-\sqrt{1-e_1^2})-p\sqrt{1-e_2^2}+p\right) \quad (34)$$

Equation (31) implies that n_1 always increases with time corresponding to inward migration. Notably this equation does not depend on the order of the resonance.

Equation (32) governs the evolution of the eccentricities. It indicates that when $e_1 = e_2 = 0$, given that the derivative de_2/de_1 remains finite, the eccentricities will increase with time provided that $1/t_{mig1} > 1/t_{mig2}$. This is just the condition for the migration of the uncoupled two planet system to be convergent, in the sense that the relative separation should decrease. When the circularization times are finite, there is the possibility of steady state eccentricities found by equating the right hand side of (32) to zero. In the limit that they are small, the equilibrium eccentricities must thus satisfy:

$$\frac{e_1^2}{t_{c1}} + \frac{e_2^2}{t_{c2}}\frac{m_2n_1a_1}{m_1n_2a_2} - \left(\frac{e_1^2}{t_{c1}} - \frac{e_2^2}{t_{c2}}\right)f = \left(\frac{1}{t_{mig1}} - \frac{1}{t_{mig2}}\right)\frac{f}{3}, \quad (35)$$

where $f = m_2a_1/((p+1)(m_2a_1+m_1a_2))$. Note that when the migration and circularization times t_{mig} and t_c scale in the same way as the mean motions at an orbital location, the equilibrium eccentricities are independent of orbital location.

REFERENCES

Adams, F. C., Laughlin, G. 2003, *Icarus,* 163, 290
Artymowicz, P., 1993, *ApJ,* 419, 155
Brouwer, D., Clemence, G. M., 1961, *Methods of Celestial Mechanics*, Academic Press, New York
Fromang, S., Terquem, C., Balbus, S.A., 2002 *MNRAS,* 329, 18
Gladman, B., 1993 *Icarus,* 106, 247
Goldreich, P., 1965, *MNRAS,* 130, 159
Goldreich, P., Tremaine, S., 1980, *ApJ,* 241, 425
Kary, D.M., Lissauer, J.J., Greenzweig, Y., 1993, *Icarus,* 106, 288
Kley, W., 2000, *MNRAS,* 313, L47
Kley, W., Peitz, J., Bryden, G. 2004, *A&A,* 414, 735
Konacki, M., Wolszczan, A., 2003, *ApJ,* 591, L147
Lee, M.H., Peale, S.J., 2002, *ApJ,* 567, 596
Lin, D.N.C., Papaloizou, J.C.B., 1986, *ApJ,* 309, 846
Marcy, G.W., Butler, R.P., Fischer, D., Vogt, S.S.; Lissauer, J.J., Rivera, E. J., 2001, *ApJ,* 556, 296
Mayor, M., Udry, S., Naef, D., Pepe, F., Queloz, D., Santos, N. C., Burnet, M., 2004, *A&A,* 415, 391
McArthur, B.E.; Endl, M., Cochran, W.D., Benedict, G.F., Fischer, D.A., Marcy, G.W., Butler, R.P., Naef, D., Mayor, M., Queloz, D., Udry, S., Harrison, T. E., 2004, *ApJ,* 614, L81
Nelson, R. P., Papaloizou, J. C. B., Masset, F., Kley, W., 2000, *MNRAS,* 318, 18
Nelson, R.P., Papaloizou, J.C.B., 2002, *MNRAS,* 333, 26
Nelson,R.P., Papaloizou, J.C.B., 2004, *MNRAS,* 350, 849
Papaloizou J.C.B., 2003, *Cel. Mech. and Dynam. Astron.*, 87, 53
Papaloizou, J.C.B., Larwood, J.D., 2000, *MNRAS,* 315, 823
Sinclair, A. T., 1975, *MNRAS,* 171, 59
Snellgrove, M., Papaloizou, J.C.B., Nelson, R.P., 2001, *A&A,* 374, 1092
Tanaka, H., Takeuchi, T., Ward, W.R., 2002, *ApJ,* 565, 1257
Tanaka, H., Ward, W.R., 2004, *ApJ,* 602, 388
Ward, W.R., 1997, *Icarus,* 126, 261

This paper has been typeset from a TEX/ LATEX file prepared by the author.